

# The Einstein-Maxwell system in 3+1 form and initial data for multiple charged black holes

Miguel Alcubierre,<sup>1,\*</sup> Juan Carlos Degollado,<sup>1,†</sup> and Marcelo Salgado<sup>1,‡</sup>

<sup>1</sup>*Instituto de Ciencias Nucleares, Universidad Nacional Autónoma de México, A.P. 70-543, México D.F. 04510, México.*

(Dated: October 31, 2018)

We consider the Einstein-Maxwell system as a Cauchy initial value problem taking the electric and magnetic fields as independent variables. Maxwell's equations in curved spacetimes are derived in detail using a 3+1 formalism and their hyperbolic properties are analyzed, showing that the resulting system is symmetric hyperbolic. We also focus on the problem of finding initial data for multiple charged black holes assuming time-symmetric initial data and using a puncture-like method to solve the Hamiltonian and the Gauss constraints. We study the behavior of the resulting initial data families, and show that previous results in this direction can be obtained as particular cases of our approach.

PACS numbers: 03.50.De, 04.20.Ex, 04.25.D-, 04.25.dg, 04.40.Nr

## I. INTRODUCTION

One of the most important results in numerical relativity in recent years has been the successful simulation of the coalescence of two spiraling (spin or spin-less) black holes (see Refs. [1, 2] for an overview). These simulations are important since one expects black hole collisions to be among the most powerful sources of gravitational radiation. Gravitational radiation from this type of sources will presumably be measured by the next generation of interferometric gravitational observatories within the next decade or so [3]. It is therefore important to have simulations of different kind of astrophysical scenarios in order to compare with the observational results in order to reach a deeper understanding of such sources of gravitational radiation. In addition to the simulations of coalescing black holes, different authors have started to analyze collisions of extended objects (*i.e.* objects constructed with a non-zero energy momentum tensor) like neutron stars [4, 5, 6, 7, 8] or even more exotic objects like boson stars [9, 10]. Since such objects are less compact than black holes, and since their individual masses are limited, one expects that the amount of gravitational radiation emitted by the collision of these objects will be weaker relative to the two-black hole problem. However, from the numerical point of view, such scenarios are by far more challenging since hydrodynamics, microphysics or field theory are also involved. Moreover, their gravitational-wave signals can be richer in the sense that they can carry information about the internal composition (*e.g.* equation of state).

Another interesting numerical problem that one can conceive and that might have an observational counterpart is the collision of two charged black holes (TCBH). This problem is simpler than the case of two neutron stars

but perhaps more interesting than the two uncharged black hole collision. In fact, it is conceivable that if black holes in binary systems were formed by the gravitational core collapse of neutron stars or supernovae then they could have a small amount of charge. Actually, even if a black hole is originally uncharged but immersed in a uniform magnetic field (which in turn can be produced by an accreting plasma surrounding the black hole), it can be charged up to some extent [11]. Very likely their charge would be small compared with their mass (in suitable units), but perhaps large enough to leave an imprint in the wave forms of gravitational radiation during a collision. In fact, numerical simulations of electromagnetic fields immersed in the background spacetime corresponding to the collision of two uncharged black holes already show that the dynamics of the background spacetime induce the emission of electromagnetic radiation that is correlated in a very particular way with the gravitational-wave signals [12]. Such electromagnetic radiation (if detected) might provide information about the pre-merger stage as a precursor to the coalescence of the black holes. One can expect that taking into account the back-reaction of the electromagnetic field in the spacetime itself can have even more interesting features.

But even from the theoretical point of view, it seems important to analyze the interplay between the gravitational and electromagnetic forces in a TCBH collision. Indeed, the analysis of the interplay between electromagnetism and gravity within a BH spacetime has a long history in general relativity [48]. The first analytic solution to Einstein's equations involving an electromagnetic field was given by Reissner and Nordström [13, 14]. This solution was interpreted as a spacetime containing a static and spherically symmetric charged black hole. Much more later, Papapetrou [15] and Majumdar [16] found a static solution involving multiple black holes having the maximal charge-to-mass ratios (see Sec. III B). Perjes [17], and Israel and Wilson [18] generalized this solution to the stationary case. Several uniqueness theorems within the Einstein-Maxwell theory have been es-

---

\*Electronic address: malcubi@nucleares.unam.mx

†Electronic address: jcdegollado@nucleares.unam.mx

‡Electronic address: marcelo@nucleares.unam.mx

tablished during the past which show how to characterize certain kind of stationary black hole solutions (see Ref. [19] for a review).

More recently, Ruffini and collaborators [20] have analyzed the case of a static charge in a Reissner-Nordström spacetime by using a perturbative approach. In the framework of the so-called *membrane paradigm* [21], and using a 3+1 formalism, Thorne and colleagues have dealt with different problems involving electromagnetic fields in strong gravitational background fields (namely those generated by stationary black holes). Such a “membrane” viewpoint allows one to approximate several results concerning electromagnetic fields around BH’s, notably at the horizons. The membrane viewpoint assigns to the horizon thermodynamic, mechanical and electric properties. In this direction one can mention the pioneering work of Damour [22] and Znajek [23], who analyzed the boundary conditions of electromagnetic fields at the horizons of a BH. Such boundary conditions can be thought of as arising from the physical properties of a fictitious membrane residing at the horizon or near the horizon (see [21] for the introduction of the notion of “stretched horizon” which allows to approximate these boundary conditions near the true horizon). Since in this viewpoint one neglects the back-reaction of the matter fields into the spacetime, this approximation will break down in situations where the self-gravity of the matter is important. It is in this regime where numerical relativity becomes crucial.

In the context of multiple charged black holes, the work by Bowen [24] was one of the first to address the initial data problem. He considered the case of zero initial magnetic field, but without imposing a moment of time-symmetry and without resorting to electromagnetic potentials. We will often make reference to Bowen’s work in this paper. Previous to Bowen’s work, Lindquist [25] generated initial data for many stationary charged particles by imposing time-symmetry and using a method of images and electromagnetic potentials. The present paper is similar in spirit to Bowen’s work, except that we shall mainly be interested in a TCBH initial data which is computed using a method analogous to the puncture method [26] which is not inversion symmetric (see Sec. III).

In order to tackle the problem of a TCBH collision there are many challenges, both numerical and analytical. First, from the numerical point of view there are two main considerations: one is the initial data and another one is the evolution of the Einstein-Maxwell system. For the former one requires suitable initial data compatible with the constraint equations. Whereas for the latter one needs a numerical code to solve the Einstein-Maxwell evolution system together with all the numerical tools necessary to analyze the location of horizons, the amount of emission of gravitational and electromagnetic radiation, etc.

As regards the analytical challenges, there are various issues with different levels of complexity. Since the vast

majority of numerical relativists are concerned with the 3+1 formulation of Einstein equations and their corresponding numerical solution, the first step toward our goal consists in obtaining a well defined 3+1 decomposition of Maxwell’s equations in a curved spacetime. It turns out that this problem has been embraced in the past in at least two works: first by Ellis in [27], and later by Thorne & Macdonald in [28]. In Section II we present a completely independent derivation of the 3+1 Maxwell equations which we then compare with the one reported by Thorne & Macdonald. Our derivation is based primary in the 3+1 formulation considered by York [29] (see Refs. [30, 31] for a thorough review of this formulation). As we will show, the 3+1 Maxwell equations in curved spacetime are in fact very similar to the usual Maxwell equations in flat spacetime, except for the fact that some extra terms due to the curvature arise. We obtain two “scalar” constraint equations for the electric and magnetic fields, and two “vector” evolution equations for those fields. In this case, the electric and magnetic fields are referred to the so-called *Eulerian* observers whose four-velocity is orthogonal to the space-like hypersurfaces that define the foliation of the four dimensional spacetime (see Sec. II). The advantage of this 3+1 formulation of Maxwell equations, as opposed to the one based on electromagnetic potentials, is that their fundamental variables are gauge invariant *ab-initio*. Therefore, one needs to focus only in the gravitational gauge issue. Moreover, the set of equations turns out to be manifestly hyperbolic (symmetric hyperbolic). The only difference with respect to the flat case is that the eigenvalues and eigenvectors associated with the principal part of the equations include contributions due to the (densitized) lapse and shift. We analyze these aspects in Sec. II A.

As we mentioned above, another challenge which can be both numerical and analytical concerns the initial data. Let us recall that in the case of the two uncharged BH collision one can consider a rich family of interesting initial conditions. The simpler ones consist on imposing a moment of time symmetry in which the two BH are initially at rest and without angular momentum and spin. With such a condition the momentum constraints are satisfied trivially. In this case, the initial data will generate a head-on collision. Moreover, one can assume that the 3-metric is conformally flat. Both conditions in the Hamiltonian constraint lead to an elliptic equation for the conformal factor (see Sec. III A). A unique solution of that equation is obtained when imposing suitable boundary conditions which in turn are related to the topology of the initial hypersurface  $\Sigma_0$  (see Refs. [30, 32] for a pedagogical review on initial data). One possible topology for  $\Sigma_0$  is  $\mathbb{R}^3$  minus two balls (the boundary of which represent the horizons of the two BH). This kind of initial data has been used in the so-called excised approach where one ignores what is inside those balls while evolving the rest of the spacetime. A simpler topology for  $\Sigma_0$  is to consider  $\mathbb{R}^3$  minus two “points”. This is the

so-called ‘‘puncture data’’ approach. The punctures represent in fact two different asymptotically flat regions on a two-throat shaped spacelike  $\Sigma_0$ . Since in vacuum the elliptic equation for the conformal factor is indeed linear one can in fact construct puncture data that represent an arbitrary number of black holes that are initially at rest. This data has a simple analytical expression whose form resemble the electric potential generated by a series of point charges.

A much more realistic initial data was the one used in the simulations of the coalescence of two binary BH that we alluded above. In this case, there is a remarkable analytical solution (the Bowen-York solution) of the momentum constraints which represents two BH with arbitrary linear momentum and spin [33]. This solution is constructed using a conformal and transverse-traceless decomposition [32]. The most difficult part of this approach is to solve a highly non-linear elliptic equation for the conformal factor. Again, one can adopt the puncture or the excised approach. In either case one needs to solve the elliptic equation numerically. The puncture approach has been very popular recently and is the one that has led to many successful evolutions of different BH binary configurations. The outcome of such evolutions has led to the prediction of a large variety of gravitational wave forms that in the near future will be confronted with the observational data [3].

Returning now to the case of the two-charged BH problem, one can take advantage of the experience with the uncharged case in order to construct interesting initial data. Unlike the uncharged case, the new difficulty is that the Einstein constraint equations will have contributions due to the electromagnetic fields. In order to simplify the problem the first attempt consists in assuming again a moment of time symmetry where the magnetic field is zero. As mentioned before, this kind of initial data was considered in the past by Bowen [24]. In this case the Poynting vector (which is the source of the momentum constraints) becomes identically zero. We could then use the Bowen-York initial data for this problem. However, one still needs to solve the Hamiltonian constraint plus the Gauss constraint for the electric field, the former containing now the contribution due to the electrostatic energy-density associated with the initial electric field generated by the two-charged BH. One can further simplify the problem if one assumes that the two BH are initially at rest (zero spin and zero linear and angular momentum). This initial data would then represent the head-on collision of two charged BH. However, unlike the vacuum case, the elliptic equation for the conformal factor is now highly non-linear. Remarkably, we have found a way to solve analytically both constraints (the Hamiltonian and Gauss constraints) using a puncture approach (see Sec. III B). This solution represents a superposition of multiple charged black holes all of which having the same charge-to-mass ratio. When this last condition is dropped, finding an analytical solution seems difficult. However, it is not difficult to find numerical solutions

(see Sec. III C).

The paper is organized as follows: Section II presents our derivation of the 3+1 Maxwell equations in a curved spacetime, as well as the analysis of their hyperbolic properties (this section is complemented by an Appendix). The Einstein-Maxwell system is summarized and a brief discussion on the electromagnetic potentials is also included. In Section III we analyze the initial data for multiple black holes using a conformal approach, where both analytical and numerical results are obtained. Finally Section IV contains several comments and remarks for the future.

## II. THE MAXWELL EQUATIONS IN 3+1 FORM

In the following we assume that the reader is familiar with the 3+1 formalism of general relativity (see Refs. [29, 30, 31], for a thorough review, and [34] for the conventions adopted here).

Let us first remember that the covariant Maxwell equations read

$$\nabla_a F^{ab} = -4\pi j^b, \quad (2.1)$$

$$\nabla_a F^{*ab} = 0, \quad (2.2)$$

where

$$F_{ab} = \partial_a A_b - \partial_b A_a, \quad (2.3)$$

$$F^{*ab} := -\frac{1}{2} \epsilon^{abcd} F_{cd}, \quad (2.4)$$

are the Faraday’s tensor and its dual. Here we take the convention that  $\epsilon^{0123} = -1/\sqrt{-g}$  and  $\epsilon_{0123} = +\sqrt{-g}$ , with the signature of  $g_{ab}$  taken as  $(-, +, +, +)$  [49].

In order to obtain the 3+1 decomposition of Maxwell equations from their covariant form, one has to proceed in a way very similar to the derivation of the so called Arnowitt-Deser-Misner (ADM) equations of General Relativity. Let us briefly review the ingredients of this decomposition. One considers a spacetime  $(M, g_{ab})$  (assumed to be globally hyperbolic) which is foliated by a family of spacelike hypersurfaces  $\Sigma_t$  ( $t \in \mathbb{R}$ ) parametrized by a global time function  $t$  (*i.e.*  $M$  has topology  $M = \Sigma_t \times \mathbb{R}$ ). The foliation is achieved in the following way: On a Cauchy surface  $\Sigma_t$ , one is given an initial data set that satisfies some constraint equations (see Sec. II C). The full spacetime is ‘‘reconstructed’’ by evolving these initial data using a suitable set of evolution equations (which includes the gauge). Such a set of constraints and evolution equations are known as the ADM equations of General Relativity.

In order to find a similar set of equations for the electromagnetic case, an analogous algebraic and geometric decomposition of the field equations (2.1) and (2.2) has to be performed. The general procedure for obtaining a 3+1 splitting of a system of covariant field equations (also called *orthogonal decomposition*) consists on projecting the different tensor fields in the directions parallel and orthogonal to the timelike unit vector field  $n^a$

( $n^a n_a = -1$ ) which is normal to  $\Sigma_t$ . The projection onto  $\Sigma_t$  is performed by first defining the *projector operator*:

$$h_b^a = \delta_b^a + n^a n_b . \quad (2.5)$$

This tensor field has the property of being idempotent:  $h_a^c h_c^b = h_a^b$ .

A tensor field  ${}^3T^{a_1 a_2 \dots a_k}_{b_1 b_2 \dots b_l}$  is said to be tangential to  $\Sigma_t$  if, when contracted with  $n^a$  it gives zero, or equivalently if contracted with  $h_b^a$  it remains unchanged. For brevity, such tensors will be termed 3-tensors. Any tensor field can be decomposed *orthogonally* by using  $h_b^a$  and  $n^a$ . In particular, a 4-vector  $w^a$  is decomposed as follows

$$w^a = {}^3w^a + w_\perp n^a , \quad (2.6)$$

where  ${}^3w^a := h_b^a w^b$  and  $w_\perp := -n_c w^c$ . Moreover, the 3+1 splitting of the metric reads

$$ds^2 = -(N^2 - N^i N_i) dt^2 - 2N_i dt dx^i + h_{ij} dx^i dx^j , \quad (2.7)$$

where the *lapse* function  $N > 0$  is defined as to normalize the (future pointing) dual vector field  $n_a = -N \nabla_a t$ . The shift vector is given by  $N^a := -h_b^a t^b$ , where  $t^a = (\partial/\partial t)^a$  is a vector field that represents the ‘‘flow’’ of the time lines and which satisfies  $t^a \nabla_a t = 1$ . This means that  $t^a$  is orthogonally decomposed as  $t^a = -N^a + N n^a$ , with  $N = -n_a t^a$ . Here  $h_{ij}$  is the 3-metric (or induced metric) of the manifold  $\Sigma_t$ . In order to avoid confusion a note on notation is important at this point: many numerical relativity references (see *e.g.* [29, 30]) use  $\alpha$  and  $\beta^a$  to denote the lapse and shift instead of  $N$  and  $N^a$ , with  $\alpha = N$  and  $\beta^a = -N^a$  (do note the change in sign in the shift!).

Another important object is the extrinsic curvature of the embeddings  $\Sigma_t$  which is defined as[50]

$$K_{ab} := -\frac{1}{2} \mathcal{L}_n h_{ab} , \quad (2.8)$$

where  $\mathcal{L}_n$  stands for the Lie derivative along  $n^a$ . From the above definition one can obtain the following identity

$$K_{ab} = -h_a^c h_b^d \nabla_c n_d , \quad (2.9)$$

which shows that  $K_{ab}$  is in fact a 3-tensor field. Furthermore, its trace is given by

$$K = -\nabla_c n^c . \quad (2.10)$$

As is well known, the set  $(\Sigma_t, h_{ab}, K_{ab})$  provides the initial data for the gravitational field. This data in fact cannot be chosen freely, and has to satisfy the Einstein constraint equations (see Sec. II C).

At this point it is useful to introduce a covariant derivative operator compatible with  $h_{ab}$ . Given a 3-tensor field  ${}^3T^{a_1 a_2 \dots a_k}_{b_1 b_2 \dots b_l}$ , one defines

$$D_e {}^3T^{a_1 a_2 \dots a_k}_{b_1 b_2 \dots b_l} = h_{c_1}^{a_1} \dots h_{c_k}^{a_k} h_{b_1}^{d_1} \dots h_{b_l}^{d_l} h_e^f \nabla_f {}^3T^{c_1 c_2 \dots c_k}_{d_1 d_2 \dots d_l} , \quad (2.11)$$

where  $D_a h_{bc} \equiv 0$ . Finally, one should mention that the indices of 3-tensors can be raised and lowered with  $h^{ab}$  and  $h_{ab}$ , and also their contravariant time components are identically zero. Moreover the projector  $h_b^a$  applied to any 3-tensor field acts as a  $\delta_b^a$ .

The Maxwell equations written in the form of an initial-data (Cauchy) problem can be obtained by projecting Eqs. (2.1) and (2.2) orthogonally and tangentially to the space-like hypersurface  $\Sigma_t$  using  $n^a$  and the projector operator (2.5), respectively. Note that with respect to a local coordinate basis adapted to the foliation we have  $n_a = (-N, 0, 0, 0)$  and  $n^a = (1/N, N^i/N)$ . In particular, in a flat spacetime one has  $n_a = (-1, 0, 0, 0)$  and  $n^a = (1, 0, 0, 0)$ .

We will need to define suitable quantities associated with the electromagnetic (EM) field before proceeding with the 3+1 decomposition of the Maxwell equations. In order to do this, consider first the 3+1 decomposition of an arbitrary 2-0 tensor, say  $H^{ab}$ , which is given as follows

$$H^{ab} = {}^{(3)}H^{ab} + n^a {}^{(3)}H^{\perp b} + {}^{(3)}H^{a\perp} n^b + H^{\perp\perp} n^a n^b , \quad (2.12)$$

with

$${}^{(3)}H^{ab} := h_c^a h_d^b H^{cd} , \quad (2.13)$$

$${}^{(3)}H^{\perp b} := -n_c h^b{}_d H^{cd} , \quad (2.14)$$

$${}^{(3)}H^{a\perp} := -n_c h^a{}_d H^{dc} , \quad (2.15)$$

$$H^{\perp\perp} := n_a n_b H^{ab} . \quad (2.16)$$

For the particular case where  $H^{ab} = F^{ab}$ , the antisymmetry of  $F^{ab}$  implies that  $F^{\perp\perp} \equiv 0$ , so [51]

$$F^{ab} = {}^{(3)}F^{ab} + n^a {}^{(3)}F^{\perp b} + {}^{(3)}F^{a\perp} n^b . \quad (2.17)$$

We now define the electric and magnetic fields as measured by the *Eulerian* observers with four velocity  $n^a$  in the following way [52]

$$E^a := -n_b F^{ba} \equiv {}^{(3)}F^{\perp a} , \quad (2.18)$$

$$B^a := -n_b F^{*ba} \equiv {}^{(3)}F^{*\perp a} . \quad (2.19)$$

The last equalities in Eqs. (2.18) and (2.19) result by noticing that the above definitions and the antisymmetry of  $F^{ab}$  and  $F^{*ab}$  both imply that  $E^a$  and  $B^a$  are in fact 3-vector fields since  $n_a E^a \equiv 0 \equiv n_a B^a$ , or equivalently  $E^a = h^a{}_d E^d$ ,  $B^a = h^a{}_d B^d$ . Otherwise such equalities can be corroborated simply by inserting Eq. (2.17) and its corresponding dual in the definitions above. In this way, one finds that

$$F^{ab} = {}^{(3)}F^{ab} + n^a E^b - E^a n^b . \quad (2.20)$$

On the other hand, from Eqs. (2.19), (2.4) and (2.20) we

have

$$\begin{aligned}
B^a &= \frac{1}{2} n_b \epsilon^{abcd} F_{cd} \\
&= \frac{1}{2} n_b \epsilon^{abcd} \left( {}^{(3)}F_{cd} + n_c E_d - E_c n_d \right) \\
&= \frac{1}{2} n_b \epsilon^{abcd} {}^{(3)}F_{cd}, \tag{2.21}
\end{aligned}$$

where in the last equality we used the fact that the contraction of the totally antisymmetric Levi-Civita symbol  $\epsilon^{abcd}$  with the symmetric tensors  $n_b n_d$  and  $n_b n_c$  vanishes identically. Moreover

$$\begin{aligned}
B^a &\equiv h^a_e B^e = \frac{1}{2} n_b h^a_e \epsilon^{becd} {}^{(3)}F_{cd} \\
&= \frac{1}{2} n_b h^a_e h_c^f h_d^g \epsilon^{becd} {}^{(3)}F_{fg} \\
&= \frac{1}{2} {}^{(3)}\epsilon^{\perp afg} {}^{(3)}F_{fg}, \tag{2.22}
\end{aligned}$$

where

$${}^{(3)}\epsilon^{\perp afg} := n_b h^a_e h_c^f h_d^g \epsilon^{becd} \equiv n_b \epsilon^{bafg}. \tag{2.23}$$

The last identity arises when using Eq. (2.5) in the above definition, plus the fact that all the contractions between  $\epsilon^{abcd}$  and more than one factor  $n_a$  vanish identically [53].

Now, since  $\epsilon^{0123} = -1/\sqrt{-g} = -1/(N\sqrt{h})$ , where  $h := \det(h_{ij})$  and  ${}^{(3)}\epsilon^{\perp afg} = -N h^a_e h_c^f h_d^g \epsilon^{0ecd}$ , it is clear that  ${}^{(3)}\epsilon^{\perp 123} = -N \epsilon^{0123} = 1/\sqrt{h}$ . Therefore we simply identify

$${}^{(3)}\epsilon^{afg} = {}^{(3)}\epsilon^{\perp afg}, \tag{2.24}$$

with the 3-Levi-Civita symbol defined in such a way that  ${}^{(3)}\epsilon^{123} = 1/\sqrt{h}$  [54]. It is also convenient to introduce a ‘‘flat’’ Levi-Civita symbol as

$$\epsilon_F^{abc} := \sqrt{h} {}^{(3)}\epsilon^{abc}, \tag{2.25}$$

$$\epsilon_{abc}^F := \frac{1}{\sqrt{h}} {}^{(3)}\epsilon_{abc}, \tag{2.26}$$

where  $\epsilon_F^{abc}$  and  $\epsilon_{abc}^F$  take values  $(0, \pm 1)$  as in flat space.

We can also invert Eq. (2.22) as follows

$${}^{(3)}F^{ab} = {}^{(3)}\epsilon^{abc} B_c, \tag{2.27}$$

so that Eq. (2.20) now reads [55]

$$F^{ab} = {}^{(3)}\epsilon^{abc} B_c + n^a E^b - E^a n^b. \tag{2.28}$$

In the same way we can obtain the following 3+1 decomposition of  $F^{*ab}$ :

$$F^{*ab} = -{}^{(3)}\epsilon^{abc} E_c + n^a B^b - B^a n^b. \tag{2.29}$$

We note that, just as in case of flat space, the dual operation maps the electric and magnetic fields as follows:  $E_a \rightarrow B_a$ ,  $B_a \rightarrow -E_a$  [56].

We are now in the position of performing the 3+1 splitting of Maxwell equations (details can be found in the Appendix). The projection of Eqs. (2.1)–(2.2) onto  $n_a$ , after the use of Eqs. (2.28) and (2.29), leads to the initial value constraints for the electric and magnetic fields respectively:

$$D_a E^a = 4\pi\rho, \tag{2.30}$$

$$D_a B^a = 0. \tag{2.31}$$

where we remind the reader that  $D_a$  is the derivative operator compatible with  $h_{ab}$  [cf. Eq. (2.11)], and  $\rho := -n_a j^a$  is the charge density as measured by the Eulerian observer. More specifically, the covariant 3-divergence is given by

$$D_a E^a = \frac{1}{\sqrt{h}} \partial_i \left( \sqrt{h} E^i \right). \tag{2.32}$$

On the other hand, the projection of (2.1) onto  $\Sigma_t$  provides the evolution equation for the electric field (see Appendix for details):

$$\begin{aligned}
h^a_c \mathcal{L}_{\mathbf{N}} E^c &= \\
&= (D \times B)^a - (B \times a)^a + K E^a - 4\pi {}^{(3)}j^a, \tag{2.33}
\end{aligned}$$

with

$$(D \times B)^a := {}^{(3)}\epsilon^{abc} \partial_b B_c, \tag{2.34}$$

$$(B \times a)^a := {}^{(3)}\epsilon^{abc} B_b a_c, \tag{2.35}$$

$${}^{(3)}j^a := h^a_b j^b, \tag{2.36}$$

and where  $K := K^a_a$  is the trace of the extrinsic curvature given by Eq. (2.10), and  $a^c := n^a \nabla_a n^c \equiv D^c(\ln N)$  is the *acceleration* of the Eulerian observer [29, 31].

Taking the spatial components of Eq. (2.33) one finds [57]

$$\begin{aligned}
\partial_t E^i + \mathcal{L}_{\mathbf{N}} E^i &= (D \times NB)^i \\
&+ N K E^i - 4\pi N {}^{(3)}j^i, \tag{2.37}
\end{aligned}$$

where now  $\mathcal{L}_{\mathbf{N}}$  is the Lie derivative along the shift, and where we used the fact that  $(D \times NB)^i = N(D \times B)^i - N(B \times a)^i$ .

In a similar way, the projection of (2.2) onto  $\Sigma_t$  provides the evolution equation for the magnetic field

$$\partial_t B^i + \mathcal{L}_{\mathbf{N}} B^i = -(D \times NE)^i + N K B^i. \tag{2.38}$$

A self-consistency check of Eq. (2.37) can be performed by noting that Eq. (2.1) implies the charge conservation equation

$$\nabla_c j^c = 0. \tag{2.39}$$

This equation can be written in terms of the 3+1 language as follows (see Appendix):

$$\partial_t \rho + \mathcal{L}_{\mathbf{N}} \rho = -D_a (N {}^{(3)}j^a) + N \rho K. \tag{2.40}$$

Therefore, by replacing in the above equation the values of  $\rho$  and  ${}^{(3)}j^c$  given by the Eqs. (2.30) and (2.37) respectively, one finds (after some algebra that involves the use of the commutator of covariant derivatives applied to a vector field as well as the Gauss-Codazzi equations) an identity. In a similar way, one can also check the self-consistency of Eqs. (2.31) and (2.38).

At this point it is important to mention that a set of 3+1 Maxwell equations analogous to Eqs. (2.30), (2.31), (2.37) and (2.38), as well as the 3+1 charge conservation Eq. (2.40), were derived previously by Thorne & Macdonald in [28] using the same sign conventions but a different notation [58]. These authors in turn used the 3+1 congruence formalism of Maxwell's equations derived by Ellis [27].

It is important to note that in a flat spacetime Eqs. (2.30), (2.31), (2.37) and (2.38) reduce to the familiar form of Maxwell's equations. For the present case of a curved spacetime, one can in fact rewrite equation (2.30) in integral form as

$$\int_{\partial\Sigma_t} E^a \sqrt{h} \sigma_a d\sigma = \int_{\Sigma_t} -n_a j^a \sqrt{h} dx^1 dx^2 dx^3. \quad (2.41)$$

On the left hand side (l.h.s), one has the flux of the electric field lines across a closed two-surface lying on  $\Sigma_t$  with normal  $\sigma_a \in T_p^{\Sigma_t}$ . On the right hand side (r.h.s), one has the total charge measured by the Eulerian observers contained in the volume enclosed by the two-surface. The r.h.s is a consequence of Eq. (2.39), which implies that the total electric charge  $Q$  is conserved:

$$\begin{aligned} Q &= \int_{\Sigma_t} N j^t \sqrt{h} dx^1 dx^2 dx^3 \\ &= \int_{\Sigma_t} -n_a j^a \sqrt{h} dx^1 dx^2 dx^3 \\ &= \int_{\Sigma_t} \rho \sqrt{h} dx^1 dx^2 dx^3. \end{aligned} \quad (2.42)$$

Note that in all the above expressions there appears the proper volume element  $\sqrt{h} dx^1 dx^2 dx^3$  on  $\Sigma_t$  as measured by the Eulerian observers. A similar analysis can be done on Eq. (2.31), except that in this case there are no magnetic charges (the magnetic field lines are always closed).

As concerns the evolution equations (2.37) and (2.38), some of the extra terms appearing there are due to curvature effects plus the fact that all observables are referred to the Eulerian observers. For instance, if one uses during the evolution the so-called *maximal slicing condition* (which is defined by imposing  $K \equiv 0 \equiv \partial_t K$ ; this leads to an elliptic equation for the lapse  $N$  [cf. Eq. (2.81)]), then the terms proportional to  $NK$  on the r.h.s of Eqs. (2.37) and (2.38) vanish identically. Otherwise, those terms are present and are associated with the time variation of the proper volume elements on  $\Sigma_t$ . Now, quite independently of the choice of a particular time slicing, Thorne & Macdonald have provided geometrical interpretations of the extra terms that couple gravity with electromagnetism

in a non-trivial fashion. Such interpretations can become even clearer when writing the evolution equations in integral form [28].

### A. Hyperbolicity analysis of Maxwell's equations in curved spacetimes

The system of evolution equations (2.37) and (2.38) for the electric and magnetic fields can clearly be written as [59]

$$\partial_t \vec{u} + \mathbb{M}^i \partial_i \vec{u} = \vec{S}. \quad (2.43)$$

where  $\vec{u} = (E^i, B^i)$  are the fundamental variables and  $\mathbb{M}^i$  are the characteristic matrices along the directions  $x^i$ .

In order to gain some insight on the hyperbolic structure of Maxwell's equations, let us first focus on the case of a flat spacetime background in Cartesian coordinates and in vacuum (*i.e.* in the absence of electric charges and currents). In such a case the matrix  $\mathbb{M}^i$  is a  $6 \times 6$  block antidiagonal matrix which can be written as the following direct sum of two  $3 \times 3$  matrices:

$$\mathbb{M}^i = \mathbb{M}_{\text{up}}^i \tilde{\oplus} \mathbb{M}_{\text{low}}^i, \quad (2.44)$$

where the symbol  $\tilde{\oplus}$  means a direct sum by placing the blocks in the antidiagonal:

$$\mathbb{M}^i = \begin{pmatrix} 0 & \mathbb{M}_{\text{up}}^i \\ \mathbb{M}_{\text{low}}^i & 0 \end{pmatrix}. \quad (2.45)$$

The components of the upper and lower matrices  $\mathbb{M}_{\text{up}}^i$  and  $\mathbb{M}_{\text{low}}^i$  are given respectively by

$$\mathbb{M}_{\text{up}}^{ilm} = \epsilon_F^{ilm} \quad (1 \leq l, m \leq 3), \quad (2.46)$$

$$\mathbb{M}_{\text{low}}^{ilm} = -\epsilon_F^{ilm} \quad (1 \leq l, m \leq 3). \quad (2.47)$$

The minus “-” in Eq. (2.47) corresponds to the asymmetry in sign in the dynamic Maxwell equations (2.37) and (2.38). However, since  $\mathbb{M}_{\text{up}}^{ilm} = \mathbb{M}_{\text{low}}^{iml}$  this shows that  $\mathbb{M}^i$  is indeed symmetric [*e.g.* see Eq. (2.52)]. Therefore one concludes that the system of equations (2.37) and (2.38) are in fact *symmetric hyperbolic* and so they admit a well posed Cauchy problem.

One can further analyze the different modes of the characteristic matrix  $\mathbb{M}^i$ . Let us take first the simple case where  $E^i$  and  $B^i$  consists of plane waves moving in the ‘x’ direction so that

$$E^i = \hat{E}^i e^{i(\omega t - kx)}, \quad (2.48)$$

$$B^i = \hat{B}^i e^{i(\omega t - kx)}. \quad (2.49)$$

Equations (2.37) and (2.38) then reduce to the following algebraic system (remember that we are considering flat spacetime in vacuum)

$$\omega \hat{E}^i + \epsilon^{ijl} k_j \hat{B}^l = 0, \quad (2.50)$$

$$\omega \hat{B}^i - \epsilon^{ijl} k_j \hat{E}^l = 0. \quad (2.51)$$

The matrix  $\mathbb{M}^x$  then takes the form

$$\mathbb{M}^x = \begin{pmatrix} 0 & 0 & 0 & 0 & 0 & 0 \\ 0 & 0 & 0 & 0 & 0 & c \\ 0 & 0 & 0 & 0 & -c & 0 \\ 0 & 0 & 0 & 0 & 0 & 0 \\ 0 & 0 & -c & 0 & 0 & 0 \\ 0 & c & 0 & 0 & 0 & 0 \end{pmatrix}, \quad (2.52)$$

where  $c := k/\omega$  corresponds to the speed of light. The constraints equations (2.30) and (2.31) impose the following conditions

$$\hat{E}_x = 0 = \hat{B}_x. \quad (2.53)$$

Now, the eigenvalues of  $\mathbb{M}^x$  are  $\vec{\lambda} = (0, 0, \pm c, \pm c)$ . The eigenvalue  $\lambda = 0$  corresponds to the eigenvectors  $\vec{e}_1 = (1, 0, 0, 0, 0, 0)$  and  $\vec{e}_2 = (0, 0, 0, 1, 0, 0)$ , the eigenvalue  $\lambda = -c$  corresponds to the eigenvectors  $\vec{e}_3 = (0, -1, 0, 0, 0, 1)$  and  $\vec{e}_4 = (0, 0, 1, 0, 1, 0)$ , and the eigenvalue  $\lambda = c$  corresponds to the eigenvectors  $\vec{e}_5 = (0, 1, 0, 0, 0, 1)$  and  $\vec{e}_6 = (0, 0, -1, 0, 1, 0)$ .

The determinant of the eigenvector matrix  $\mathbb{R}^x$  is

$$\det(\mathbb{R}^x) = -4. \quad (2.54)$$

The set of eigenvectors therefore is complete, and the evolution system turns to be strongly hyperbolic. This of course is not a surprise since we already knew that  $\mathbb{M}^x$  is symmetric and therefore the system is in fact symmetric hyperbolic.

The first two modes with speed zero ( $\lambda = 0$ ) are clearly unphysical since they are associated with modes that violate the constraints (2.53). On the other hand, the modes with speed  $\pm c$  do satisfy the constraints. These physical modes correspond to  $\vec{e}_3, \vec{e}_4, \vec{e}_5, \vec{e}_6$ , and are associated with the two polarizations states (each one with speed  $\pm c$ ) of the electromagnetic waves.

Now, for the case of waves propagating along an arbitrary direction defined by the unit vector  $\vec{s}$ , the principal symbol of the system is given by  $\mathbb{C} := \mathbb{M}^i s_i$ . Then we have

$$\mathbb{C} = \begin{pmatrix} 0 & 0 & 0 & 0 & s_3 & -s_2 \\ 0 & 0 & 0 & -s_3 & 0 & s_1 \\ 0 & 0 & 0 & s_2 & -s_1 & 0 \\ 0 & -s_3 & s_2 & 0 & 0 & 0 \\ s_3 & 0 & -s_1 & 0 & 0 & 0 \\ -s_2 & s_1 & 0 & 0 & 0 & 0 \end{pmatrix}. \quad (2.55)$$

The eigenvalues are  $\vec{\lambda} = (0, 0, \pm 1, \pm 1)$  with corresponding eigenvectors (from now on we will take the speed of light to be equal to 1):

- $\lambda = 0$ :

$$\vec{e}_1 = (s_1/s_3, s_2/s_3, 1, 0, 0, 0), \quad (2.56)$$

$$\vec{e}_2 = (0, 0, 0, s_1/s_3, s_2/s_3, 1). \quad (2.57)$$

- $\lambda = -1$

$$\vec{e}_3 = (s_2, -(s_1^2 + s_3^2)/s_1, s_2 s_3/s_1, -s_3/s_1, 0, 1), \quad (2.58)$$

$$\vec{e}_4 = (-s_3, -s_2 s_3/s_1, (s_1^2 + s_2^2)/s_1, -s_2/s_1, 1, 0). \quad (2.59)$$

- $\lambda = 1$

$$\vec{e}_5 = (-s_2, (s_1^2 + s_3^2)/s_1, -s_2 s_3/s_1, -s_3/s_1, 0, 1). \quad (2.60)$$

$$\vec{e}_6 = (s_3, s_2 s_3/s_1, -(s_1^2 + s_2^2)/s_1, -s_2/s_1, 1, 0). \quad (2.61)$$

and the determinant of the eigenvector matrix  $\mathbb{R}$  is

$$\det(\mathbb{R}) = -4/(s_1^2 s_3^2). \quad (2.62)$$

The set of eigenvectors is clearly complete, and the evolution system again turns out to be strongly hyperbolic. Since  $\mathbb{C}$  is symmetric, the system is in fact symmetric hyperbolic.

Again, the two modes with zero speed violate the constraints since  $\vec{S} \cdot \vec{e}_1$  and  $\vec{S} \cdot \vec{e}_2$  do not vanish, where  $\vec{S} := (s_1, s_2, s_3, s_1, s_2, s_3)$  (the constraints correspond to  $\partial_i u^i = 0$ , that is,  $\hat{u}^i S_i = 0 = \hat{E}^i s_i + \hat{B}^i s_i$ ). On the other hand, one can see that  $\vec{S} \cdot \vec{e}_i$  vanish identically for  $i = (3, \dots, 6)$ . Therefore such modes satisfy the constraints and propagate with the speed of light. They correspond to the two polarization states with speed  $\pm 1$ .

We can now consider the full system of evolution equations (2.37) and (2.38) with a prescribed shift. The principal symbol now reads,

$$\mathbb{C} = \begin{pmatrix} N_s & 0 & 0 & 0 & \mathcal{N} s_3 & -\mathcal{N} s_2 \\ 0 & N_s & 0 & -\mathcal{N} s_3 & 0 & \mathcal{N} s_1 \\ 0 & 0 & N_s & \mathcal{N} s_2 & -\mathcal{N} s_1 & 0 \\ 0 & -\mathcal{N} s_3 & \mathcal{N} s_2 & N_s & 0 & 0 \\ \mathcal{N} s_3 & 0 & -\mathcal{N} s_1 & 0 & N_s & 0 \\ -\mathcal{N} s_2 & \mathcal{N} s_1 & 0 & 0 & 0 & N_s \end{pmatrix}. \quad (2.63)$$

where  $N_s := N^i s_i$ , and with  $\mathcal{N} := N/\sqrt{h}$  the *densitized* lapse.

The eigenvalues of the principal symbol are now  $\vec{\lambda} = (N_s, N_s, N_s \pm \mathcal{N})$ . These correspond to the characteristic speeds as measured by the Eulerian observers. In the flat spacetime limit they reduce to those previously obtained. Their corresponding eigenvectors are now

- $\lambda = N_s$

$$\vec{e}_1 = (s_1/s_3, s_2/s_3, 1, 0, 0, 0), \quad (2.64)$$

$$\vec{e}_2 = (0, 0, 0, s_1/s_3, s_2/s_3, 1). \quad (2.65)$$

- $\lambda = N_s - \mathcal{N}$

$$\vec{e}_3 = (s_2, -(s_1^2 + s_3^2)/s_1, s_2 s_3/s_1, -s_3/s_1, 0, 1). \quad (2.66)$$

$$\vec{e}_4 = (-s_3, -s_2 s_3/s_1, (s_1^2 + s_2^2)/s_1, -s_2/s_1, 1, 0). \quad (2.67)$$

- $\lambda = N_s + \mathcal{N}$

$$\vec{e}_5 = (-s_2, (s_1^2 + s_3^2)/s_1, -s_2 s_3/s_1, -s_3/s_1, 0, 1), \quad (2.68)$$

$$\vec{e}_6 = (s_3, s_2 s_3/s_1, -(s_1^2 + s_2^2)/s_1, -s_2/s_1, 1, 0). \quad (2.69)$$

Just as in the flat case, the first two modes which propagate with the coordinate speed  $N_s$  are unphysical since they violate the constraints. On the other hand, the remaining modes satisfy the constraints and propagate at the speed of light  $N_s \pm \mathcal{N}$ .

The characteristic speeds along a given direction  $x^i$  can also be written as  $\vec{\lambda}^i = (N^i, N^i, N^i \pm \mathcal{N}S^i)$ , so that the projection along the  $\vec{s}$  direction provides  $\vec{\lambda}$ . This shows that physical modes propagate along the light cones, corresponding to the coordinate speeds  $N^i \pm \mathcal{N}S^i$ .

### B. The energy-momentum tensor of the electromagnetic field

The energy-momentum tensor of the EM field is given by

$$T_{ab} = \frac{1}{4\pi} \left[ F_{ac} F_b{}^c - \frac{1}{4} g_{ab} F_{cd} F^{cd} \right]. \quad (2.70)$$

Using Eq. (2.28) we obtain

$$F_{ac} F_b{}^c = -(E_a E_b + B_a B_b) + B^2 h_{ab} + E^2 n_a n_b + 2E^c B^d {}^{(3)}\epsilon_{cd(a} n_{b)}, \quad (2.71)$$

where  $E^2 = E^a E_a$  and  $B^2 = B^a B_a$ .

From the above equation one can easily find

$$F_{ac} F^{ac} = -2(E^2 - B^2). \quad (2.72)$$

The energy-momentum tensor (2.70) then becomes

$$T_{ab} = \frac{1}{4\pi} \left[ -(E_a E_b + B_a B_b) + \frac{1}{2} h_{ab} (E^2 + B^2) + \frac{1}{2} n_a n_b (E^2 + B^2) + 2E^c B^d {}^{(3)}\epsilon_{cd(a} n_{b)} \right], \quad (2.73)$$

where we have used the fact that  $g_{ab} = h_{ab} - n_a n_b$  [cf. Eq. (2.5)]. The 3+1 decomposition of this tensor is [cf. Eq. (2.12)]

$$T_{ab} = \mathcal{E} n_a n_b + n_a J_b + J_a n_b + S_{ab}, \quad (2.74)$$

where now [cf. Eqs. (2.13)–(2.16)]

$$\mathcal{E} := n^a n^b T_{ab} = \frac{1}{8\pi} (E^2 + B^2), \quad (2.75)$$

$$J_a := -h_a{}^c n^d T_{dc} = \frac{1}{4\pi} {}^{(3)}\epsilon_{acd} E^c B^d, \quad (2.76)$$

$$S_{ab} := h_a{}^c h_b{}^d T_{cd} = \frac{1}{8\pi} [h_{ab} (E^2 + B^2) - 2(E_a E_b + B_a B_b)]. \quad (2.77)$$

We identify  $\mathcal{E}$  with the energy-density of the EM field as measured by the Eulerian observers,  $J_a$  with the momentum density measured by those observers (the *Poynting vector*), and  $S_{ab}$  with the stress tensor [60].

Since the trace  $T^a{}_a$  of the energy-momentum tensor (2.70) vanishes, then Eq. (2.74) leads to [cf. Eqs. (2.75) and (2.77)],

$$S = \mathcal{E}, \quad (2.78)$$

where  $S = S^a{}_a$  is the trace of the 3-tensor (2.77).

### C. The Einstein-Maxwell system

We now consider the Einstein equations in 3+1 form, with the matter sources provided by the electromagnetic field contributions of Sec. II B.

The Hamiltonian and momentum constraints are, respectively [29, 30, 31]

$${}^3R + K^2 - K_{ij} K^{ij} = 16\pi\mathcal{E}, \quad (2.79)$$

$$D_l K^{il} - D^i K = 8\pi J^i. \quad (2.80)$$

The dynamic Einstein equations read [29, 30, 31]

$$\begin{aligned} & \partial_t K_{ij} + \mathcal{L}_N K_{ij} + D_i D_j N \\ & - N ({}^3R_{ij} + K K_{ij} - 2K_{il} K_j{}^l) \\ & = 4\pi N [h_{ij}(S - \mathcal{E}) - 2S_{ij}] = -8\pi N S_{ij}, \end{aligned} \quad (2.81)$$

where we used Eq. (2.78) to simplify the r.h.s of Eq. (2.81). Taking now the trace in Eq. (2.81), and using Eq. (2.79), one obtains the following evolution equation which can be very useful in many cases (*e.g.* see Sec. III below):

$$\begin{aligned} & \partial_t K + N^l \partial_l K + D^2 N - N K_{ij} K^{ij} \\ & = 4\pi N (S + \mathcal{E}) = 8\pi N \mathcal{E}, \end{aligned} \quad (2.82)$$

where we used Eq. (2.78) in the last step. Here  $D^2$  stands for the Laplacian operator compatible with the 3-metric  $h_{ab}$ .

In all the four equations (2.79)–(2.82), the r.h.s is given in terms of the energy-momentum contributions defined in Eqs. (2.75)–(2.77).

It is well known that the evolution equations (2.81), when written in first order form, are only weakly hyperbolic (see Ref. [30] for a thorough review), and so do not admit a well-posed Cauchy problem (in the Hadamard sense). However, by adding suitable multiples of the constraints and using a conformal decomposition (*e.g.* the BSSN formulation [35]) one can write the evolution system in such a way that the evolution system admits a well posed Cauchy problem. Here we are not concerned with that issue, but will consider it when we study numerical evolutions of the Einstein-Maxwell system in a future paper.

The Cauchy problem in this case can be summarized as follows: given the initial data  $(\Sigma_t, h_{ab}, K_{ab}, E_a, B_a)$ , satisfying the constraints (2.79), (2.80), (2.30) and (2.31), one can then evolve forward in time (given a prescription for  $N$  and  $N^i$ ) the fields  $h_{ab}, K_{ab}, E_a, B_a$  using their evolution equations (2.8), (2.81) (or their corresponding strongly hyperbolic formulated equations), (2.37) and (2.38) respectively [61].



### D. Electromagnetic potentials

Up until this point we have worked directly with the electric and magnetic fields and ignored the potentials. This is quite deliberate, as the use of the potentials can complicate matters, in particular due to the fact that one needs to choose a gauge. Also, the evolution equations for the electromagnetic field when written in terms of the potentials are second order in space and time, which brings extra complications coming from the fact that covariant derivatives do not commute. Nevertheless, here we will very briefly describe, without going into any details, the 3+1 form of the electromagnetic potentials and their relation with the electric and magnetic fields.

Let us start by remembering that in terms of the potential 4-vector  $A^a$  the Faraday tensor is given by equation (2.3), which we rewrite here for concreteness:

$$F_{ab} = \partial_a A_b - \partial_b A_a . \quad (2.83)$$

Starting from the potential 4-vector, one can now define a 3+1 “scalar potential”  $\Phi$  through

$$\Phi := -n_a A^a , \quad (2.84)$$

together with a potential 3-vector  ${}^{(3)}A^a$  defined as

$${}^{(3)}A^a := h^a_b A^b . \quad (2.85)$$

From these definitions one can immediately find that, in a coordinate system adapted to the 3+1 foliation:

$$\Phi = N A^t = -\frac{1}{N} (A_t + N^a A_a) , \quad (2.86)$$

and

$${}^{(3)}A^a = A^a - n^a \Phi , \quad {}^{(3)}A_i = A_i . \quad (2.87)$$

Now, by projecting the expression for the Faraday tensor in terms of  $A^a$  given above one can obtain, after some algebra, the following relation between the electric-field  $E_i$  and the 3+1 potentials:

$$\partial_t {}^{(3)}A_i + \mathcal{L}_N {}^{(3)}A_i = -N E_i - D_i (N \Phi) . \quad (2.88)$$

Notice that this equation can in fact be interpreted as an evolution equation for the potential 3-vector  ${}^{(3)}A_i$ .

Similarly, one can also obtain the following expression for the magnetic field  $B_i$  in terms of  ${}^{(3)}A_i$ :

$$\begin{aligned} B^i &= \frac{1}{2} {}^{(3)}\epsilon^{imn} \left( \partial_m {}^{(3)}A_n - \partial_n {}^{(3)}A_m \right) \\ &= {}^{(3)}\epsilon^{imn} \partial_m {}^{(3)}A_n = \left( D \times {}^{(3)}A \right)^i , \end{aligned} \quad (2.89)$$

with the rotational operator  $(D \times {}^{(3)}A)$  defined in the same way as before.

At this point, one could take the point of view that the independent dynamical variables are in fact  ${}^{(3)}A^i = h^{ij} {}^{(3)}A_j$  and  $E^i$ , with evolution equations given by (2.37)

and (2.88), and simply define the magnetic field through Eq. (2.89), therefore ignoring Eq. (2.38) (which is now just a consequence of the definition of  $B^i$ ). One would also find that the magnetic constraint (2.31) is now trivial. We would then have a system of evolution equations that is first order in time and second order in space, with only one constraint, namely the electric constraint (2.30).

Of course, one would still have to choose a gauge condition in order to evolve the scalar potential  $\Phi$ . One possibility would be to take the *Lorentz gauge*, which is given in terms of the 4-vector potential as:

$$\nabla_a A^a = 0 . \quad (2.90)$$

This gauge condition can be easily seen to take the following form in 3+1 language

$$\partial_t \Phi + \mathcal{L}_N \Phi = -D_m \left( N {}^{(3)}A^m \right) + N K \Phi , \quad (2.91)$$

with  $K$  the trace of the extrinsic curvature, which clearly provides us with an evolution equation for  $\Phi$ .

Taking this point of view, however, has one serious drawback. One can show that the system of evolution equations given by (2.37), (2.88) and (2.91) is in fact only weakly hyperbolic even in flat space (*i.e.* it has real eigenvalues, but does not have a complete set of eigenvectors), so that the system is not well-posed. There are certainly ways around this, involving defining new auxiliary variables and *crucially* commuting the second covariant derivatives of  ${}^{(3)}A^i$  that would appear in Eq. (2.37) when we write the magnetic field as (2.89) (which considerably complicates the equation by bringing in a contribution from the Riemann tensor), but we will not go into such details here (see *e.g.* Ref. [36]). It is enough to say that, even though strongly hyperbolic versions of the evolution system for  ${}^{(3)}A^i$  and  $E^i$  do exist, it is simpler and much cleaner to work with the electric and magnetic fields directly, and consider the potentials just as auxiliary variables when (and if) they are needed.

### III. INITIAL DATA FOR MULTIPLE CHARGED BLACK HOLES

In this Section we will consider the problem of finding suitable initial data for multiple charged black holes. For simplicity, will concentrate on the case of time-symmetric initial data for which the extrinsic curvature vanishes  $K_{ab} = 0$ . Furthermore, we will also assume that the initial magnetic field is zero, in which case the momentum constraints are identically satisfied.

The problem of solving the Einstein-Maxwell constraint equations was studied previously by Bowen in [24], where he used a method of images (notably for the electric field) to construct a manifold that represents two isometric asymptotically flat universes with  $n$  throats connecting them. In that work Bowen describes a solution for the electric field that is inversion symmetric

through the throats (but which do not arise from a potential), which then allows one to find numerical initial data for the 3-metric that represents  $n$  charged black holes. Here, however, we will use a different approach and will look instead for solutions that are not inversion symmetric, but that rather represent a series of throats that connect our universe to  $n$  *distinct* asymptotically flat universes, more in the spirit of the Brill-Lindquist [37] initial data for time-symmetric black holes, or the Brandt-Bruegmann [26] puncture data for spinning or moving black holes.

### A. Conformal transformation of the metric and electric field

For time symmetric initial data and vanishing magnetic field, the problem of finding initial data reduces to finding a solution of the electric constraint (2.30)

$$D_a E^a = 4\pi\rho, \quad (3.1)$$

together with the Hamiltonian constraint (2.79)

$${}^3R = 16\pi\mathcal{E}, \quad (3.2)$$

with the energy density of the EM given by:

$$\mathcal{E} = \frac{1}{8\pi} E_a E^a. \quad (3.3)$$

Let us now assume that the spatial metric  $h_{ab}$  is conformally flat, so that we can rewrite it as:

$$h_{ab} = \psi^4 \hat{h}_{ab}, \quad (3.4)$$

with  $\psi$  the conformal factor and  $\hat{h}_{ab}$  a flat background metric in arbitrary coordinates. The Hamiltonian constraint then reduces to the following elliptic equation for the conformal factor

$$\hat{D}^2\psi + \frac{1}{4}\psi^5 E_a E^a = 0, \quad (3.5)$$

with  $\hat{D}^2$  the Laplacian operator compatible with the background metric.

With the above conformal transformation in mind, let us now consider the electric constraint (3.1). Notice first that  $D_a$  is the derivative operator associated with the physical metric  $h_{ab}$ . Notice also that, quite generally, for any vector  $v^a$  we have

$$D_a v^a = \hat{D}_a v^a + 6v^a \partial_a \ln \psi, \quad (3.6)$$

with  $\psi$  the conformal factor introduced above and  $\hat{D}$  the derivative operator associated with the conformal metric  $\hat{h}_{ab}$ . This implies in particular that

$$D_a (\psi^n v^a) = \psi^n \left[ \hat{D}_a v^a + (6+n)v^a \partial_a \ln \psi \right]. \quad (3.7)$$

Using this result it is then natural to define the conformally rescaled electric field as

$$\hat{E}^a := \psi^6 E^a, \quad \hat{E}_a := \psi^2 E_a, \quad (3.8)$$

and the conformally rescaled charge density as

$$\hat{\rho} := \psi^6 \rho. \quad (3.9)$$

The electric constraint then reduces to

$$\hat{D}_a \hat{E}^a = 4\pi\hat{\rho}, \quad (3.10)$$

where now the divergence is calculated with respect to the conformal metric.

In terms of the conformal electric field just defined, the Hamiltonian constraint takes the final form:

$$\hat{D}^2\psi + \frac{1}{4\psi^3} \hat{E}_a \hat{E}^a = 0. \quad (3.11)$$

In order to find initial data, one must then first solve the conformal electric constraint (3.10), and then plug in the solution for  $\hat{E}^a$  into the Hamiltonian constraint in order to solve for the conformal factor  $\psi$ .

In fact, Eq. (3.11) can also be written as

$$\bar{\psi} \hat{D}^2 \bar{\psi} - \frac{1}{2} (\hat{D}^a \bar{\psi}) (\hat{D}_a \bar{\psi}) + \frac{1}{2} \hat{E}_a \hat{E}^a = 0. \quad (3.12)$$

where  $\bar{\psi} := \psi^2$ . This equation was considered by Bowen [24] for solving the initial data for the single charged black hole case (see the analysis below).

### B. Exact initial data multiple charged black holes with the same charge-to-mass ratio

In order to find initial data for multiple charged black holes we will first assume that the background metric is flat. Let us introduce a conformal electric potential  $\varphi$  such that

$$\hat{E}_a = -\partial_a \varphi. \quad (3.13)$$

Do notice that the conformal potential  $\varphi$  does not coincide with the physical potential  $\Phi$  discussed in Sec. II D above, since even in the absence of a vector potential equation (2.88) clearly shows that the relation between  $\Phi$  and the physical electric field involves the lapse function.

Using Eq. (3.13), the electric constraint can be rewritten as

$$\hat{D}^2\varphi = -4\pi\hat{\rho}. \quad (3.14)$$

From now on we will also assume that we are in a region away from any charges, so that  $\hat{\rho} = 0$ .

Before attempting to find initial data for multiple charged black holes, let us recall for a moment the Reissner-Nordström analytic static solution for a single

charged black hole with mass  $M$  and charge  $Q$  [13, 14], for which the conformal electric potential  $\varphi$  and the conformal factor  $\psi$  are given by:

$$\varphi = \frac{Q}{r}, \quad \psi = \left[ \left(1 + \frac{M}{2r}\right)^2 - \frac{Q^2}{4r^2} \right]^{1/2}, \quad (3.15)$$

where we have assumed that the black hole is centered on the origin of the coordinate system  $r = 0$ .

The conformal and physical electric fields for this solution are purely radial and are given by:

$$\hat{E}^r = \frac{Q}{r^2}, \quad E^r = \frac{Q}{r^2 \psi^6}. \quad (3.16)$$

The fact that the conformal factor  $\psi$  above is an exact solution of Eq. (3.11) for this electric field can be verified by direct substitution.

Since in this case the spacetime is static, Eq. (2.82) provides a linear elliptic equation for the lapse:

$$\hat{D}^2 N = 8\pi N \mathcal{E} = N E^a E_a, \quad (3.17)$$

which in terms of the conformal variables reads

$$\hat{D}^2 N + \frac{2}{\psi} (\hat{D}^i N) (\hat{D}_i \psi) = \frac{N}{\psi^4} \hat{E}_a \hat{E}^a. \quad (3.18)$$

One can now also confirm by direct substitution that the lapse given by Eq. (3.19) below solves Eq. (3.18) when using in turn Eqs. (3.15) and (3.16):

$$N = \frac{(1 + M/2r)(1 - M/2r) + Q^2/4r^2}{(1 + M/2r)^2 - Q^2/4r^2}. \quad (3.19)$$

Notice that Eqs. (3.15), (3.16) and (3.19) correspond to the Reissner-Nordström solution in isotropic (*i.e.* conformally flat) coordinates, and not in the standard Schwarzschild-like coordinates one finds in most text books [62]. It is clear that by taking  $Q \equiv 0$ , the above solution reduces to the Schwarzschild solution in isotropic coordinates.

Based on the form of the conformal factor for the Reissner-Nordström solution given above, we will now propose the following *ansatz* for the conformal factor in the presence of a generic electric potential  $\varphi$  that is a solution of the electric constraint (3.14):

$$\bar{\psi} = \psi^2 = (1 + \eta)^2 - \frac{\varphi^2}{4}. \quad (3.20)$$

Substituting this back into equation (3.12) we find, after some algebra, the following elliptic equation for  $\eta$ :

$$(1 + \eta) \left( (1 + \eta)^2 - \frac{\varphi^2}{4} \right) \hat{D}^2 \eta - \frac{\varphi^4}{4} \partial_m \left( \frac{\eta}{\varphi} \right) \partial^m \left( \frac{\eta + 2}{\varphi} \right) = 0, \quad (3.21)$$

where we have already used the fact that  $\hat{D}^2 \varphi = 0$ .

We can now easily notice a remarkable fact: If we take the function  $\eta$  to be proportional to the electric potential  $\varphi$ , that is  $\eta = k\varphi$  for some constant  $k$ , then equation (3.12) is identically satisfied since in such a case we clearly have  $\partial_m (\eta/\varphi) = 0$  and  $\hat{D}^2 \eta = 0$  (remember that  $\varphi$  solves the electric constraint away from charges).

We will now use this fact to find an exact solution of the Hamiltonian constraint for multiple black holes. Let us assume that in the conformal space we have a series of point charges with values  $Q_i$  located at the points  $\vec{r}_i$ . The solution for the potential  $\varphi$  is then clearly

$$\varphi = \sum_{i=1}^n \frac{Q_i}{|\vec{r} - \vec{r}_i|}. \quad (3.22)$$

Let us now choose  $\eta$  proportional to  $\varphi$  in the following way:

$$\eta = k\varphi = k \sum_{i=1}^n \frac{Q_i}{|\vec{r} - \vec{r}_i|} \equiv \sum_{i=1}^n \frac{M_i}{2|\vec{r} - \vec{r}_i|}. \quad (3.23)$$

We can now construct a conformal factor that satisfies the Hamiltonian constraint as in (3.20):

$$\psi^2 = \left( 1 + \sum_{i=1}^n \frac{M_i}{2|\vec{r} - \vec{r}_i|} \right)^2 - \frac{1}{4} \left( \sum_{i=1}^n \frac{Q_i}{|\vec{r} - \vec{r}_i|} \right)^2, \quad (3.24)$$

with  $M_i = 2kQ_i$ , and  $k$  an arbitrary constant. This solution represents a series of  $n$  charged black holes, all of which have *the same charge-to-mass ratio*  $Q_i/M_i = 1/2k$ .

One could ask at this point how can we know that the above solution in fact does represent a series of black holes. There are several ways to see that this should be so. First, notice that if we take  $n = 1$  this is just the standard Reissner-Nordström solution for a single charged black hole. Second, in the case when all the charges vanish the conformal factor (3.24) above reduces to the well known Brill-Lindquist conformal factor for a series of non-charged black holes [37]. Also, if the different points  $\vec{r}_i$  are very far apart, then close to each of them the conformal factor again reduces essentially to the Reissner-Nordström solution, so we would indeed have a series of  $n$  charged black holes. Finally, notice that because of the singularities in the conformal factor, as we approach each point  $\vec{r}_i$  the areas of spheres centered around that point first become smaller and then increase again. That is, our initial data is a topological construction with a series of wormholes connecting to other asymptotically flat regions. Since the initial data is time symmetric the throats of these wormholes (*i.e.* the minimal surfaces) in fact correspond to apparent horizons. Of course, if some of the points  $\vec{r}_i$  are very close to each other one could find common apparent horizons around them, so that we actually have fewer black holes with complicated internal topologies. As a final comment, notice also that due to the tidal forces between the different black holes, the throats of the wormholes can not be expected to be

spherical, and their precise shape and location should be found numerically.

That an exact solution of the Hamiltonian constraint for multiple charged black holes exists at all is a surprising result. Notice, however, that we have only found a solution for the *initial data*. In general, one would expect this initial configuration to evolve as each black hole reacts to the gravitational and electric fields of the other black holes, so that a non-zero extrinsic curvature and magnetic field would quickly develop.

There is in fact one notable exception to this. In order to find it we will first rewrite the conformal factor (3.24) in the following way

$$\psi^2 = 1 + 2k \sum_{i=1}^n \frac{Q_i}{|\vec{r} - \vec{r}_i|} + \left(k^2 - \frac{1}{4}\right) \left(\sum_{i=1}^n \frac{Q_i}{|\vec{r} - \vec{r}_i|}\right)^2, \quad (3.25)$$

where we have already used the fact that  $M_i = 2k Q_i$ . If we now take  $k = 1/2$ , which implies  $M_i = Q_i$ , then the conformal factor reduces to:

$$\psi^2 = 1 + \sum_{i=1}^n \frac{Q_i}{|\vec{r} - \vec{r}_i|}, \quad (3.26)$$

which now corresponds to initial data for a series of *extremal* black holes. Amazingly, one can show that this multi-extremal black hole solution turns out to be static, that is, the gravitational attraction of all the black holes is *exactly canceled out* by their electrostatic repulsion, so that the black holes never move from their initial positions. The lapse function for such a static solution is given by:

$$N = 1/\psi^2 = \left[1 + \sum_{i=1}^n \frac{Q_i}{|\vec{r} - \vec{r}_i|}\right]^{-1}. \quad (3.27)$$

which solves Eq. (3.18) exactly.

This multi-extremal static solution was first obtained by Papapetrou [15] and Majumdar [16] (see [19] for a review), and was further analyzed by several authors [17, 18, 38, 39, 40] [63]. This solution is so well known that it can even be found in some text books (see *e.g.* the recent book by Carroll [41]). On the other hand, as far as we are aware the exact solution of the Hamiltonian constraint for non-extremal black holes with equal charge-to-mass ratios presented above was not previously known.

### C. Numerical initial data for multiple charged black holes with different charge-to-mass ratios

The exact multiple black hole solution of the Hamiltonian constraint found in the previous section is only valid in the case when all the black holes have the same

charge-to-mass ratio. When considering different charge-to-mass ratios we have not been able to find a closed form solution. On the other hand, finding numerical solutions can be done easily enough. In order to do this we will first modify our ansatz (3.20) above in the following way:

$$\bar{\psi} = \psi^2 = (u + \eta)^2 - \frac{\varphi^2}{4}, \quad (3.28)$$

with

$$\eta = \sum_{i=1}^N \frac{M_i}{2|\vec{r} - \vec{r}_i|}, \quad (3.29)$$

$$\varphi = \sum_{i=1}^N \frac{Q_i}{|\vec{r} - \vec{r}_i|}, \quad (3.30)$$

and where  $u$  is a function that goes to 1 at infinity, and in fact is identically equal to 1 everywhere in the case when all charge-to-mass ratios are equal.

Substituting now Eq. (3.28) into the Hamiltonian constraint we find the following elliptic equation for  $u$ :

$$(\eta + u) \left( (\eta + u)^2 - \frac{\varphi^2}{4} \right) \hat{D}^2 u - \frac{\varphi^4}{4} \partial_m \left( \frac{\eta + u - 1}{\varphi} \right) \partial^m \left( \frac{\eta + u + 1}{\varphi} \right) = 0, \quad (3.31)$$

The above equation needs to be solved numerically for  $u$  in the case when the charge-to-mass ratios of the different black holes are not all equal.

Before presenting some examples of numerical solutions for the case of two black holes, it is important to investigate the expected behaviour of the function  $u$  close to each of the ‘‘punctures’’, that is, close to each of the points  $\vec{r} = \vec{r}_i$ . In order to do this, let us now use a system of spherical coordinates  $(r, \theta, \phi)$  adapted to one of the black holes. Without loss of generality we will choose that black hole as the one identified with the label 1, so that  $\vec{r}_1 = 0$ . Let us now examine the behavior of the different terms in equation (3.31) for small  $r$ . Consider first the coefficient of the Laplacian operator:

$$T_1 := (\eta + u) \left( (\eta + u)^2 - \frac{\varphi^2}{4} \right). \quad (3.32)$$

Let us assume for the moment that  $u$  is finite at each of the punctures. From the form of the functions  $\eta$  and  $\varphi$ , it is then clear that for small  $r$  this term behaves in general as

$$T_1 \sim 1/r^3. \quad (3.33)$$

Consider now the term with first order derivatives in Eq. (3.31):

$$T_2 := \varphi^4 \partial_m \left( \frac{\eta + u - 1}{\varphi} \right) \partial^m \left( \frac{\eta + u + 1}{\varphi} \right). \quad (3.34)$$

In order to analyze the behaviour of this term for small  $r$ , we will first expand the derivatives to obtain

$$T_2 = [\varphi \partial_m(\eta + u) - (\eta + u - 1) \partial_m \varphi] [\varphi \partial^m(\eta + u) - (\eta + u + 1) \partial^m \varphi]. \quad (3.35)$$

We will now rewrite the functions  $\eta$  and  $\varphi$  above as

$$\eta = \frac{M_1}{2r} + H(r, \theta, \phi), \quad \varphi = \frac{Q_1}{r} + F(r, \theta, \phi), \quad (3.36)$$

with  $H$  and  $F$  given by

$$H = \sum_{i \neq 1} \frac{M_i}{2|\vec{r} - \vec{r}_i|}, \quad F = \sum_{i \neq 1} \frac{Q_i}{|\vec{r} - \vec{r}_i|}, \quad (3.37)$$

which are clearly regular functions at  $r = 0$ . Substituting into  $T_2$  and expanding we find, after some algebra, that for small  $r$  this term behaves as:

$$T_2 \sim 1/r^4. \quad (3.38)$$

Notice that naively one could expect  $T_2$  to diverge as  $1/r^6$ , due to the presence of terms of the form  $(\varphi \partial_r \eta)^2$ , but in fact all such terms cancel out and we are left with a dominant divergence of order  $1/r^4$ .

From the behaviour of  $T_1$  and  $T_2$  for small  $r$ , we then find that in order for equation (3.31) to be consistent the Laplacian of  $u$  must behave for small  $r$  as:

$$\hat{D}^2 u \sim 1/r. \quad (3.39)$$

Now, in spherical coordinates the (flat) Laplacian is given by

$$\hat{D}^2 u = \partial_r^2 u + \frac{2}{r} \partial_r u + \frac{1}{r^2} L^2 u, \quad (3.40)$$

with  $L^2$  the angular operator

$$L^2 u := \frac{1}{\sin \theta} \partial_\theta (\sin \theta \partial_\theta u) + \frac{1}{\sin^2 \theta} \partial_\varphi^2 u. \quad (3.41)$$

This implies that in order to have  $\hat{D}^2 u$  behaving as expected for small  $r$  we must ask for the function  $u$  to have a Taylor expansion near the origin of the form:

$$u = a + b(\theta, \phi) r, \quad (3.42)$$

with  $a$  a constant and  $b(\theta, \phi)$  some regular function of the angular coordinates. Notice that  $b(\theta, \phi)$  *must* be non-zero for equation (3.31) to be consistent, so the above expansion implies that  $u$  is not regular at the origin (remember that  $r$  is a radial coordinate). The function  $u$  then turns out to be only  $C^0$  at the punctures, that is, it is finite and continuous, but its derivatives are no longer continuous. In other words, the function  $u$  is in general expected to have a kink (*i.e.* a conical singularity) at each of the punctures (we will see in the numerical examples below that this is indeed the case).

#### D. Numerical examples for the case of two charged black holes

We have constructed a simple numerical code to solve equation (3.31) for the case of two charged black holes with different charge-to-mass ratios. In such a case one can locate both black holes along the  $z$  axis. The situation is then clearly axisymmetric, so the problem is effectively two-dimensional.

As a boundary condition we ask for the function  $u$  to behave as  $u = 1 + c/r$  for large  $r$ , where  $r = \sqrt{\rho^2 + z^2}$  and  $c$  is some constant. In order to eliminate the unknown constant this boundary condition is differentiated and applied in the following way:

$$\partial_r u = \frac{1 - u}{r}. \quad (3.43)$$

Our code uses cylindrical coordinates  $(\rho, z, \phi)$  instead of spherical coordinates  $(r, \theta, \phi)$ , so that in practice we assume that far away the dependence on the azimuthal angle  $\theta$  can be ignored, so that one can write

$$\partial_\rho u = \left(\frac{\rho}{r}\right) \partial_r u, \quad \partial_z u = \left(\frac{z}{r}\right) \partial_r u. \quad (3.44)$$

The final boundary condition on the  $\rho$  boundaries is then

$$\left(\frac{r}{\rho}\right) \partial_\rho u = \frac{1 - u}{r}, \quad (3.45)$$

with an analogous condition on the  $z$  boundaries.

Since here we are mainly interested in showing that the solutions for  $u$  can be easily found and that they behave as expected, we have decided to write a very simple code that instead of solving the elliptic equation directly solves an associated hyperbolic problem of the form:

$$\begin{aligned} \partial_t^2 u &= \hat{D}^2 u - \frac{\varphi^4}{4} \partial_m \left(\frac{\eta + u - 1}{\varphi}\right) \partial^m \left(\frac{\eta + u + 1}{\varphi}\right) \\ &\times \left[ (\eta + u) \left( (\eta + u)^2 - \frac{\varphi^2}{4} \right) \right]^{-1}, \end{aligned} \quad (3.46)$$

with  $t$  a fictitious time parameter. The boundary conditions are then also modified to outgoing-wave boundary conditions of the form:

$$\partial_t u + \left(\frac{r}{\rho}\right) \partial_\rho u = \frac{1 - u}{r}, \quad (3.47)$$

and analogously for the  $z$  boundaries. We choose as initial condition  $u = 1$ , and evolve the above hyperbolic equation until we reach a stationary state with some predetermined tolerance. The idea is that the wave-like equation above will propagate the residual away through the boundaries, and will drive the system to a static solution which corresponds to the solution of the original elliptic problem.

Spatial derivatives are approximated with standard centered second order differences, while for the time integration we use a three-step iterative Crank-Nicholson

algorithm [42, 43]. The resulting code is rather slow, particularly for high resolutions, but has the advantage of being both very simple to write (and debug), and also extremely robust. A more sophisticated elliptic solver should of course be used in order to find highly accurate solutions in a short computational time (we certainly do not recommend to use our quick-and-dirty “wave-like” algorithm for any kind of production runs).

In order to deal with the problem of divisions by  $\rho$  our computational grid staggers the axis and introduces a ghost grid point at position  $\rho = -\Delta\rho/2$ . To determine the value of  $u$  at this ghost point we then simply impose the parity condition  $u(-\Delta\rho/2) = u(\Delta\rho/2)$ .

Notice that we don’t do anything special close to the punctures and just take standard centered differences everywhere. This clearly affects the order of convergence close to the punctures (see numerical examples below).

### 1. Example I: Equal masses and opposite charges

As a first example we will consider the case of black holes with equal masses  $M_1 = M_2 = 1$ , and equal but opposite charges  $Q_1 = -Q_2 = 1/2$ . The punctures are located along the  $z$  axis at positions  $z_1 = -z_2 = 2$  and the boundaries extend to  $\rho = 6$ ,  $z = \pm 6$ .

As initial guess we choose  $u = 1$  everywhere, and then evolve equation (3.46) until the magnitude of right hand side is everywhere smaller than a fixed tolerance of  $\epsilon = 10^{-8}$ . This tolerance is chosen such that it is always smaller than the truncation error at the resolutions considered here.

Figure 1 shows the numerical solution for the function  $u$  along the  $z$  axis, for a resolution of  $\Delta\rho = \Delta z = 0.01$ . Notice how the function  $u$  behaves as expected on both punctures, with very evident kinks. One can also see that  $u$  has equatorial symmetry even though the charges have opposite signs. Of course, had we chosen both charges with the same sign the exact solution would have been  $u = 1$  everywhere since in that case the charge-to-mass ratios would have been equal. It is also interesting to note that the maximum deviation of the function  $u$  from unity is precisely at the punctures, and this maximum deviation is of only about 7%. Figure 2 shows the a height map of the same solution in the  $(\rho, z)$  plane.

Next we show a plot of the convergence in the Hamiltonian constraint along the  $z$  axis. Since we are in fact solving numerically precisely the Hamiltonian constraint, one would expect it to be satisfied to the level of the tolerance in the elliptic solver. This is of course true, but in order to study convergence we are in fact using a different expression for the Hamiltonian constraint. We first reconstruct the conformal factor  $\psi$ , and later evaluate numerically to second order the Hamiltonian constraint (3.11) written as:

$$\hat{D}^2\psi + \frac{1}{4\psi^3} \partial_m\varphi \partial^m\varphi = 0. \quad (3.48)$$

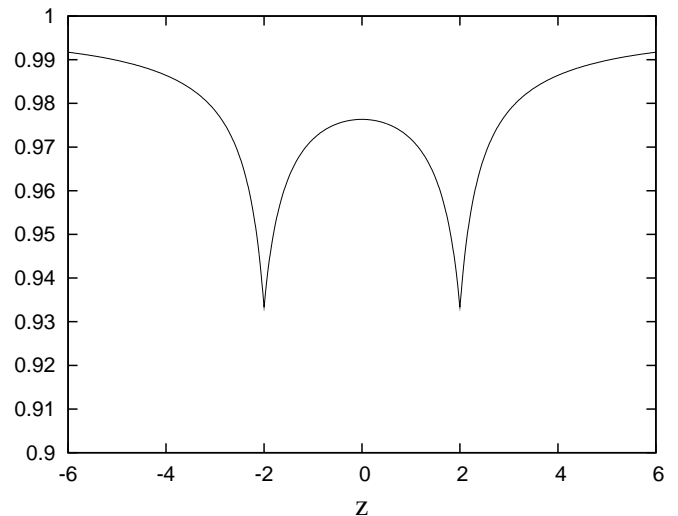


FIG. 1: Numerical solution for the function  $u$  along the  $z$  axis for the case of equal masses and equal but opposite charges.

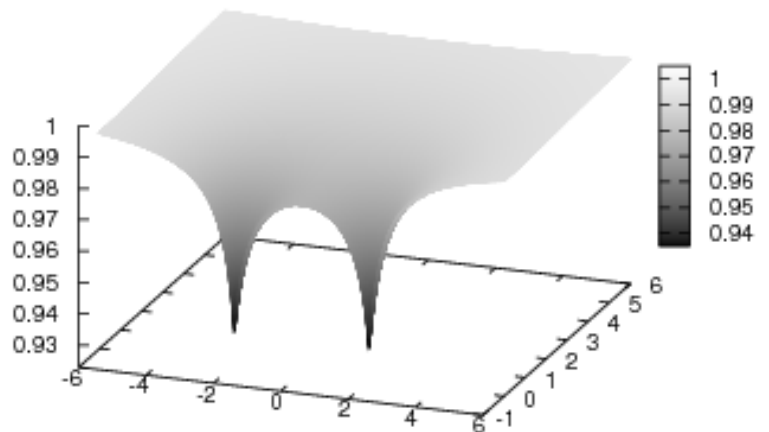


FIG. 2: Height map in the  $(\rho, z)$  plane of the numerical solution for the function  $u$ .

This last expression should not be expected to hold to the level of the tolerance in the elliptic solver, but rather to the level of numerical truncation error, which is much higher (we have chosen a very small tolerance parameter in the elliptic solver precisely for this reason).

Figure 3 shows the logarithm of the absolute value of the Hamiltonian constraint evaluated using (3.48) for the five different resolutions  $\Delta\rho = \Delta z = 0.1, 0.05, 0.025, 0.0125, 0.00625$ , with each plot rescaled by the corresponding factor expected for second order convergence: 1, 4, 16, 64, 256 (we in fact show only the region close to one of the punctures as the situation is symmetric on the other puncture). Notice how away from the

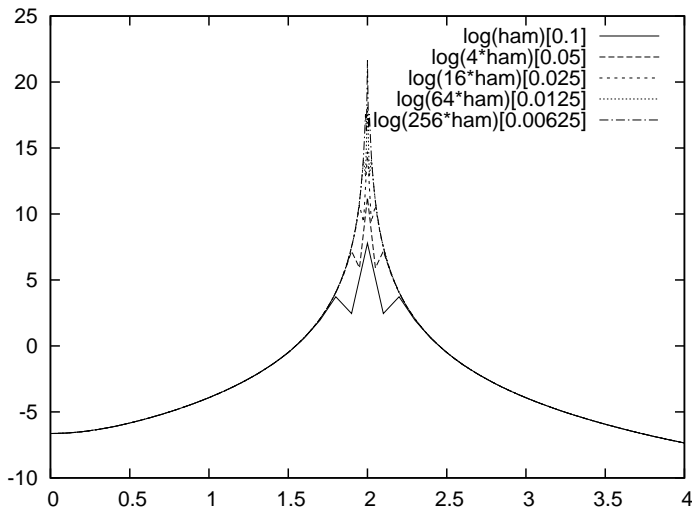


FIG. 3: Convergence of the Hamiltonian constraint. We plot the logarithm of the absolute value of the Hamiltonian constraint evaluated at 5 different resolutions, with each resolution rescaled by the corresponding factor in order to show second order convergence.

puncture all plots lie on top of each other, showing nice second order convergence. Closer to the puncture, however, the Hamiltonian constraint in fact increases with higher resolution, but this loss of convergence is limited to the 2 or 3 grid points closest to the puncture, so that the non-converging region keeps getting smaller and smaller with higher resolution. This should not be surprising since in the conformal factor  $\psi$  we have terms that diverge as  $1/r$  close to each puncture.

### 2. Example II: Equal masses and one charge equal to zero

As a second example we will consider the case of two black holes with equal masses  $M_1 = M_2 = 1$ , and one charge set equal to zero  $Q_1 = 1/2$ ,  $Q_2 = 0$ . As before, the punctures are located along the  $z$  axis at positions  $z_1 = -z_2 = 2$  and we use a resolution of  $\Delta\rho = \Delta z = 0.0125$ . The results are plotted in Figure 4. Notice that even though  $Q_2 = 0$ , the function  $u$  still has a small kink at  $z = -2$ .

### 3. Example III: Some more generic cases

As a more generic case we set up two black holes with different masses,  $M_1 = 1, M_2 = 0.5$ , located as before at the points  $z_1 = -z_2 = 2$ . The first black hole has a charge of  $Q_1 = 1/2$ , while for the charge of the second black hole we consider a series of values:  $Q_2 = -0.25, -0.1, 0.0, 0.1, 0.25$ . The results are plotted in Figure 5.

What seems to happen as  $Q_1 > 0$  is kept fixed and

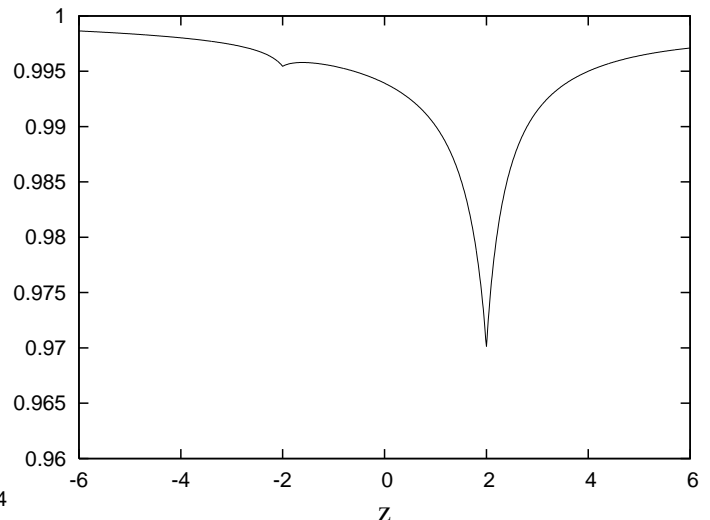


FIG. 4: Similar to Fig. 1, but for the case of equal masses and one charge equal to zero.

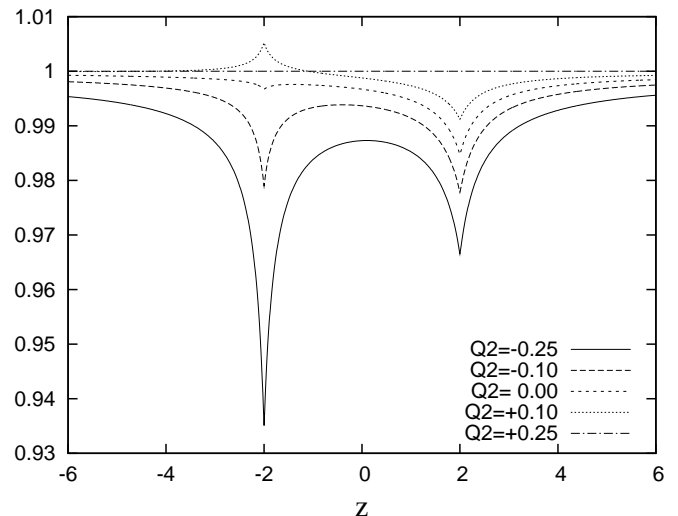


FIG. 5: Similar to Fig. 1 for a more generic case in which the back hole at  $z = 2$  has  $M_1 = 1$ ,  $Q_1 = 1/2$ , while for the black hole at  $z = -2$  we take  $M_2 = 1/2$  and a series of values for the charge:  $Q_2 = -0.25, -0.1, 0, 0.1, 0.25$ .

$Q_2$  changes is that, for  $Q_2 < 0$ , the kinks in  $u$  are point down at both punctures. Then, as  $Q_2$  approaches zero the kink at that puncture becomes much smaller but still keeps pointing down. If  $Q_2$  goes through zero and becomes positive, then the kink at  $z_2$  first disappears and later starts growing again in the opposite direction. As  $Q_2$  keeps increasing towards a value where both charge-to-mass ratios are equal both kinks become smaller with opposite directions, until the function  $u$  becomes 1 everywhere.

By trial and error we have in fact found a situation for which the kink at  $z = -2$  seems to essentially disappear. Figure 6 shows the numerical solution for  $u$  in the case

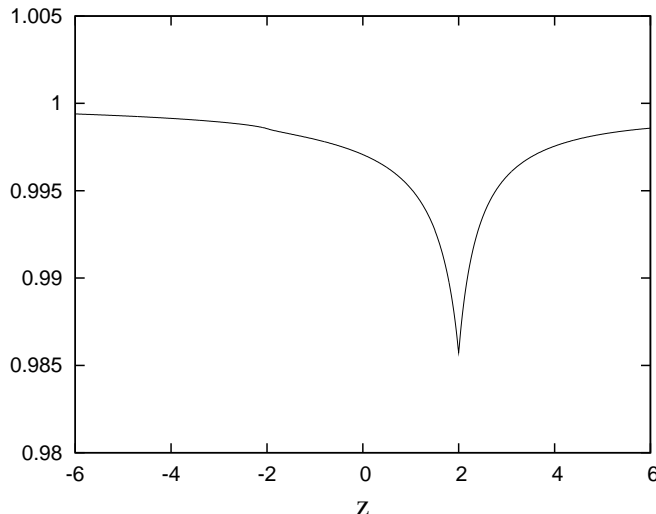


FIG. 6: Solution for  $u$  in the case when  $M_1 = 1, M_2 = 0.5, Q_1 = 0.5, Q_2 = 0.01475$ . Notice that the kink at  $z = -2$  is essentially gone.

when  $M_1 = 1, M_2 = 0.5, Q_1 = 0.5, Q_2 = 0.01475$ .

The special value of  $Q_2$  for which the kink disappears can in fact be estimated analytically. When we examined the behaviour of the function  $u$  near the punctures in Section III C above, we mentioned the fact the source term of equation (3.31), which we called  $T_2$ , behaves as  $1/r^4$  near each puncture. Being somewhat more precise one can show that for the case of two black holes this term behaves close to the puncture at  $\vec{r}_2$  as

$$\begin{aligned}
 T_2 &= \frac{1}{4r^4} \left( \frac{Q_1 M_2}{d} - \frac{Q_2 M_1}{d} - 2Q_2 \Delta u \right) \\
 &\times \left( \frac{Q_1 M_2}{d} - \frac{Q_2 M_1}{d} - 4Q_2 - 2Q_2 \Delta u \right) \\
 &+ \mathcal{O}(1/r^3), \tag{3.49}
 \end{aligned}$$

with  $r = |\vec{r} - \vec{r}_2|$ , and where  $d$  is the distance between the punctures and  $\Delta u = u(\vec{r}_2) - 1$ . Notice that there are two ways in which the term  $T_2$  can vanish, corresponding to a solution  $u$  that is regular at the puncture. One possibility is to have  $u = 1$ , so that  $\Delta u = 0$ , and equal charge-to-mass ratios so that  $Q_1 M_2 = Q_2 M_1$ , in which case the first term above vanishes. This is clearly the exact solution we already described. But a second possibility is to assume that  $u$  is very close to 1 at the puncture so that  $\Delta u \ll 1$ , and to ask for  $Q_2 \sim Q_1 M_2 / (M_1 + 4d)$ , in which case the second term above will almost vanish ( $T_2$  will in fact not vanish exactly for this value of  $Q_2$  since at the puncture  $\Delta u$  is not exactly zero, but one can expect  $T_2$  to vanish for a value of  $Q_2$  that is very close to this one). For the values in our example we have  $M_1 = 1, M_2 = 0.5, Q_1 = 0.5$  and  $d = 4$ , so that  $Q_2 \sim 1/68 \sim 0.0147$ , which is remarkably close to the empirical value found above.

## IV. CONCLUSIONS

We have considered the Einstein-Maxwell system having two goals in mind. The first goal consisted in recasting the covariant Maxwell equations in a curved spacetime as an initial value problem along the lines of the usual 3+1 formalism of general relativity, choosing the magnetic and electric fields as independent variables. This led to a set of two constraint equations for the electric and magnetic fields, plus a set of two evolution equations for those fields. The evolution equations are hyperbolic with the propagation speeds depending on the lapse and shift.

The second goal was to construct initial data satisfying the gravitational and electromagnetic constraints which represent momentarily static charged black holes. In order to achieve this goal we assumed a moment of time symmetry with vanishing extrinsic curvature and magnetic field. For the case of two black holes, this initial data will serve to analyze a head-on collision. We found that for black holes having an equal charge-to-mass ratio it is possible to find an analytic solution for the constraints. However, when this condition is dropped, we present instead numerical solutions. We studied the behavior of such solutions with several values of the free parameters (*i.e.* different masses and charges), showing extremal cases.

A much more realistic initial data will consist in relaxing the moment of time symmetry condition (*i.e.* abandon the initial condition  $K_{ij} = 0$ ), but keeping a null initial magnetic field and analyze the analogous of the Bowen-York initial data. In this case, one will need to solve a much more complex Hamiltonian constraint for the conformal factor. An elliptic solver will be required *a fortiori* to solve this constraint. This is an issue that is worth analyzing in the future.

Using the initial data presented here we plan in a near future to study the evolution of the Einstein-Maxwell system generated by the collision of two charged black holes, and analyze the emission of both gravitational and electromagnetic radiation. We believe that the interplay between gravity and electromagnetism will give rise to very interesting and unusual dynamics due to the possibility of repulsion between charges. This is an issue that has not been scrutinized thus far in numerical relativity.

## Acknowledgments

This work was supported in part by Dirección General de Estudios de Posgrado (DGEP-UNAM), by CONACyT through grant 82787, and by DGAPA-UNAM through grant IN113907. JCD also acknowledges CONACyT support.



## APPENDIX

For the sake of clarity, we will give here some details about our derivation of the 3+1 Maxwell equations. We start with Eq. (2.1). The projection of this equation onto  $n_a$  reads:

$$n_b \nabla_a F^{ab} = 4\pi\rho, \quad (1)$$

where one must remember  $\rho := -n_b j^b$ . At this point there are several possible ways to proceed. Let us first write

$$\begin{aligned} n_b \nabla_a F^{ab} &= \nabla_a (n_b F^{ab}) - F^{ab} \nabla_a n_b \\ &= \nabla_a E^a - F^{ab} \nabla_a n_b, \end{aligned} \quad (2)$$

where in the last step we used Eq. (2.18).

Now, concerning the term  $\nabla_a E^a$ , one way to relate it with 3+1 quantities is by using the following identity for any 4-vector field  $V^a$

$$\begin{aligned} \nabla_a V^a &= \frac{1}{\sqrt{-g}} \partial_a (\sqrt{-g} V^a) \\ &= \frac{1}{N\sqrt{h}} \partial_a (N\sqrt{h} V^a), \end{aligned} \quad (3)$$

where we have used the fact that  $g = -N^2 h$ . We then have

$$\nabla_a V^a = V^a \partial_a \ln N + \frac{1}{\sqrt{h}} \partial_a (\sqrt{h} V^a). \quad (4)$$

For the particular case where  $V^a = E^a$ , it turns out that  $E^a \partial_a \ln N = E^b h_b^a \nabla_a \ln N = E^a D_a \ln N$ , where the fact that  $E^a \equiv E^b h_b^a$  is a consequence of the fact that  $E^a$  is a 3-vector. Moreover, since  $E^t \equiv 0$  the term  $(1/\sqrt{h}) \partial_a (\sqrt{h} E^a)$  reduces to the 3-divergence  $D_a E^a$ . We then have

$$\nabla_a E^a = D_a E^a + E_a a^a, \quad (5)$$

where we used the following identity for the acceleration of the Eulerian observer  $a_b := n^a \nabla_a n_b \equiv D_b \ln N$ . We point out that one could have obtained the same result from the definition of the 3-covariant divergence:

$$\begin{aligned} D_a E^a &= h_a^c h_b^a \nabla_c E^b = h_b^c \nabla_c E^b = \nabla_b E^b + n^c n_b \nabla_c E^b \\ &= \nabla_b E^b + n^c \nabla_c (n_b E^b) - n^c E^b \nabla_c n_b \\ &= \nabla_b E^b - E^b a_b. \end{aligned} \quad (6)$$

where we used the fact that  $n_b E^b \equiv 0$  since  $E^a$  is by definition orthogonal to  $n^a$ . From this equation one obtains the same identity (5). Using this result Eq. (2) now reads

$$n_b \nabla_a F^{ab} = D_a E^a + E_a a^a - F^{ab} \nabla_a n_b. \quad (7)$$

We now need to prove that, in fact,  $F^{ab} \nabla_a n_b = E_a a^a$ . For this we use Eq. (2.20) to obtain

$$F^{ab} \nabla_a n_b = {}^{(3)}F^{ab} \nabla_a n_b + n^a E^b \nabla_a n_b - E^a n^b \nabla_a n_b. \quad (8)$$

The second term in the last equation is precisely  $n^a E^b \nabla_a n_b = E^b a_b$ , while the third vanishes identically since  $n^b n_b = -1$ , and therefore  $\nabla_a (n^b n_b) = 2n^b \nabla_a n_b \equiv 0$ . Finally, we show that the first term vanishes by using the definition of the extrinsic curvature, Eq. (2.8):

$${}^{(3)}F^{ab} K_{ab} = -{}^{(3)}F^{ab} h_a^c h_b^d \nabla_c n_d = -{}^{(3)}F^{cd} \nabla_c n_d. \quad (9)$$

This term vanishes identically because  ${}^{(3)}F^{ab}$  is antisymmetric while  $K_{ab}$  is symmetric. We have thus proved that  $F^{ab} \nabla_a n_b = E_a a^a$ . Using this result in Eq. (7) allows us to conclude that

$$n_b \nabla_a F^{ab} = D_a E^a = 4\pi\rho. \quad (10)$$

Following an analogous procedure, one can now also obtain Eq (2.31) by projecting Eq. (2.2), except that one now uses Eq. (2.29) instead of (2.20). In this case, there is no magnetic charge.

We proceed now to obtain Eq. (2.37) by projecting (2.1) onto  $\Sigma_t$  using  $h^a_b$ :

$$h^a_b \nabla_c F^{cb} = -4\pi {}^{(3)}j^a. \quad (11)$$

Using Eq. (2.20) and expanding we obtain

$$\begin{aligned} h^a_b \nabla_c {}^{(3)}F^{cb} - E^c h^a_b \nabla_c n^b + E^a \nabla_c n^c + h^a_b n^c \nabla_c E^b \\ = h^a_b \nabla_c {}^{(3)}F^{cb} + E^b K_b^a - E^a K + h^a_b n^c \nabla_c E^b \\ = -4\pi {}^{(3)}j^a. \end{aligned} \quad (12)$$

where we used  $E^c h^a_b \nabla_c n^b = E^d h_d^c h^a_b \nabla_c n^b = -E^d K_d^a$ , and  $K = -\nabla_c n^c$  [cf. Eqs. (2.9) and (2.10)].

Now, from the definition of the 3-covariant derivative applied to a 3-tensor field we have [cf. Eq. (2.11)]

$$\begin{aligned} D_c {}^{(3)}F^{cb} &= h_c^d h_e^c h_b^f \nabla_d {}^{(3)}F^{ef} = h_c^d h_b^f \nabla_d {}^{(3)}F^{ef} \\ &= h_b^f \nabla_d {}^{(3)}F^{df} - {}^{(3)}F^{eb} \nabla_d (n_e n^d) \\ &= h_b^f \nabla_d {}^{(3)}F^{df} - {}^{(3)}F^{eb} a_e. \end{aligned} \quad (13)$$

In this way Eq. (12) becomes

$$\begin{aligned} h^a_b n^c \nabla_c E^b + D_c {}^{(3)}F^{ca} + {}^{(3)}F^{ba} a_b \\ + E^b K_b^a - E^a K = -4\pi {}^{(3)}j^a. \end{aligned} \quad (14)$$

The first term above can be rewritten using the following identities

$$\begin{aligned} h^a_b \mathcal{L}_n E^b &= h^a_b (n^c \nabla_c E^b - E^c \nabla_c n^b) \\ &= h^a_b n^c \nabla_c E^b + K^a_c E^c. \end{aligned} \quad (15)$$

We then conclude that

$$\begin{aligned} h^a_b \mathcal{L}_n E^b + D_c {}^{(3)}F^{ca} + {}^{(3)}F^{ba} a_b \\ - E^a K = -4\pi {}^{(3)}j^a. \end{aligned} \quad (16)$$

Finally, using the fact that  ${}^{(3)}F^{ca}$  is antisymmetric, together with Eqs. (2.27) and (2.25), one can write

$$\begin{aligned} D_c {}^{(3)}F^{ca} &= \frac{1}{\sqrt{h}} \partial_i \left( \sqrt{h} {}^{(3)}F^{ia} \right) = \frac{1}{\sqrt{h}} \partial_b \left( \epsilon_F^{bac} B_c \right) \\ &= \frac{\epsilon_F^{bac}}{\sqrt{h}} \partial_b B_c = -{}^{(3)}\epsilon^{abc} \partial_b B_c . \end{aligned} \quad (17)$$

Equation (16) then reads

$$\begin{aligned} h^a_b \mathcal{L}_n E^b - {}^{(3)}\epsilon^{abc} \partial_b B_c + {}^{(3)}\epsilon^{abc} B_b a_c \\ - E^a K = -4\pi {}^{(3)}j^a , \end{aligned} \quad (18)$$

where we used again Eq. (2.27) to rewrite the third term. Taking the notation given by Eqs. (2.34) and (2.35), one finally recovers Eq. (2.33).

In order to find Eq. (2.37) from Eq. (18), one has to remember that the Lie derivative can be written in terms of ordinary derivatives as follows

$$h^a_b \mathcal{L}_n E^b = h^a_b \left( n^c \partial_c E^b - E^c \partial_c n^b \right) . \quad (19)$$

Now, since we are only interesting in the spatial components of Eq. (18), using (2.5) together with  $n_a = (-N, 0, 0, 0)$ ,  $n^a = (1/N, N^i/N)$  one can easily show that

$$h^i_a \mathcal{L}_n E^a = \frac{1}{N} \partial_t E^i + \frac{N^j}{N} \partial_j E^i - \frac{E^j}{N} \partial_j N^i . \quad (20)$$

Substituting this last result into the spatial components of (18) leads directly to Eq. (2.37).

In a similar fashion one can obtain Eq. (2.38) by projecting (2.2) onto  $\Sigma_t$ . In fact, this just amounts to using the duality relations  $E_a \rightarrow B_a$  and  $B_a \rightarrow -E_a$  in (2.37) to obtain Eq. (2.38).

Finally, we proceed to derive Eq. (2.40). This can be easily done by using the orthogonal decomposition of the electric-current 4-vector [cf. Eq. (2.6)]:

$$j^a = {}^{(3)}j^a + \rho n^a , \quad (21)$$

being  $\rho := -n_a j^a$  the charge density measured by the Eulerian observer, and  ${}^{(3)}j^a := h^a_c j^c$ . This decomposition, when inserted into Eq. (2.39) and making use of (2.10), leads directly to

$$n^a \nabla_a \rho - \rho K + \nabla_a {}^{(3)}j^a = 0 . \quad (22)$$

Using now Eq. (5) for  ${}^{(3)}j^a$  instead of  $E^a$  (the expression is valid for any 3-vector), one obtains

$$\mathcal{L}_n \rho + D_a {}^{(3)}j^a + {}^{(3)}j^a a_a - \rho K = 0 , \quad (23)$$

where

$$\mathcal{L}_n \rho \equiv n^a \nabla_a \rho = 1/N \left( \partial_t \rho + N^j \partial_j \rho \right) . \quad (24)$$

- 
- [1] F. Pretorius, in *Relativistic Objects in Compact Binaries: From Birth to Coalescence*, edited by M. Colpi *et al.* (Springer, Heidelberg, Germany, 2009).
- [2] M. Hannam, *Class. Quantum Grav.* **26**, 114001 (2009).
- [3] B. A. *et al.*, (2009), gr-qc/0901.4399.
- [4] K. Kiuchi, Y. Sekiguchi, M. Shibata, and K. Taniguchi, (2009).
- [5] B. Giacomazzo, L. Rezzolla, and L. Baiotti, (2009).
- [6] M. Anderson *et al.*, *Phys. Rev. Lett.* **100**, 191101 (2008), gr-qc/0801.4387.
- [7] M. Anderson *et al.*, *Phys. Rev. D* **77**, 024006 (2008), gr-qc/0708.2720.
- [8] L. Baiotti, B. Giacomazzo, and L. Rezzolla, *Phys. Rev. D* **78**, 084033 (2008).
- [9] C. Palenzuela, L. Lehner, and S. L. Liebling, *Phys. Rev. D* **77**, 044036 (2008).
- [10] C. Palenzuela, I. Olabarrieta, L. Lehner, and S. L. Liebling, *Phys. Rev. D* **75**, 064005 (2007).
- [11] R. M. Wald, *Phys. Rev. D* **10**, 1680 (1974).
- [12] C. Palenzuela *et al.*, (2009), astro-ph/0905.1121.
- [13] H. Reissner, *Ann. Phys.* **50**, 106 (1916).
- [14] G. Nordström, *Proc. Kon. Ned. Akad. Wet.* **20**, 1238 (1918).
- [15] A. Papapetrou, *Proc. R. Irish Acad.* **A51**, 191 (1945).
- [16] S. D. Majumdar, *Phys. Rev.* **72**, 390 (1947).
- [17] Z. Perjés, *Phys. Rev. Lett.* **27**, 1668 (1972).
- [18] W. Israel and G. A. Wilson, *J. Math. Phys.* **13**, 865 (1972).
- [19] M. Heusler, *Black Hole Uniqueness Theorems* (Cambridge University Press, Cambridge, England, 1996).
- [20] D. Bini, A. Geralico, and R. Ruffini, *Phys. Rev. D* **75**, 044012 (2007).
- [21] K. S. Thorne, R. H. Price, and D. A. Macdonald, *The Membrane Paradigm* (Yale University Press, New Haven, 1986).
- [22] T. Damour, *Phys. Rev. D* **18**, 3598 (1978).
- [23] R. L. Znajek, *Mon. Not. Roy. Astron. Soc.* **185**, 833 (1978).
- [24] J. M. Bowen, *Ann. of Phys.* **165**, 17 (1985).
- [25] R. W. Lindquist, *J. Math. Phys.* **4**, 938 (1963).
- [26] S. Brandt and B. Brügmann, *Phys. Rev. Lett.* **78**, 3606 (1997), gr-qc/9703066.
- [27] G. Ellis, in *Cargèse lectures in Physics*, edited by E. Schatzman (Gordon & Breach, New York, USA, 1973).
- [28] K. S. Thorne and D. Macdonald, *Mon. Not. R. Astr. Soc.* **198**, 339 (1982).
- [29] J. York, in *Sources of Gravitational Radiation*, edited by L. Smarr (Cambridge University Press, Cambridge, England, 1979).
- [30] M. Alcubierre, *Introduction to 3+1 Numerical Relativity* (Oxford Univ. Press, New York, 2008).
- [31] E.ourgoulhon, (2007), gr-qc/0703035.

- [32] E.ourgoulhon, J.Phys.Conf.Ser. **91**, 012001 (2007), gr-qc/0704.0149.
- [33] J. M. Bowen and J. W. York, Phys. Rev. D **21**, 2047 (1980).
- [34] R. M. Wald, *General Relativity* (The University of Chicago Press, Chicago, U.S.A., 1984).
- [35] T. W. Baumgarte and S. L. Shapiro, Phys. Rev. **D59**, 024007 (1998).
- [36] A. M. Knapp, E. J. Walker, and T. W. Baumgarte, Phys. Rev. **D65**, 064031 (2002).
- [37] D. Brill and R. Lindquist, Phys. Rev. **131**, 471 (1963).
- [38] J. B. Hartle and S. W. Hawking, Commun. Math. Phys. **26**, 87 (1972).
- [39] P. T. Chruściel and N. S. Nadirashvili, Class. Quantum Grav. **12**, L17 (1994).
- [40] M. Heusler, Class. Quantum Grav. **14**, L129 (1997).
- [41] S. M. Carroll, *Spacetime and geometry: An introduction to general relativity* (Addison Wesley, San Francisco, 2004).
- [42] S. Teukolsky, Phys. Rev. D **61**, 087501 (2000), gr-qc/9909026.
- [43] M. Alcubierre *et al.*, Phys. Rev. D **62**, 044034 (2000), gr-qc/0003071.
- [44] J. A. Wheeler, Phys. Rev. **97**, 511 (1955).
- [45] J. M. Bardeen, W. H. Press, and S. A. Teukolsky, Astrophys. J. **178**, 347 (1973).
- [46] A. Lichnerowicz, *Théories Relativistes de la Gravitation et de l'Électromagnétisme* (Masson & Cie, éditeurs, Paris, France, 1955).
- [47] L. Witten, Phys. Rev. **120**, 635 (1960).
- [48] In a wider context which includes extended objects and not only black holes, such an interplay was first analyzed by Wheeler in [44]. However, here we will not be concerned with objects other than charged black holes.
- [49] A change of convention for the signs of the Levi-Civita tensor (for a left-handed as opposed to right-handed orthonormal basis), entails a change of sign in equations (2.4) and (2.21). For instance, the convention adopted in many books like Landau's *The Classical Theory of Fields* is that  $\epsilon_{0123} = -1$  and  $\epsilon^{0123} = +1$  in a left-handed orthonormal basis.
- [50] It is to note that in Wald's book (*op. cit.*) the extrinsic curvature is defined with the opposite sign.
- [51] One could define  ${}^{(3)}F_{ab} := D_a {}^{(3)}A_b - D_b {}^{(3)}A_a$  instead of  ${}^{(3)}F_{ab} := F_{cd} h_a^c h_b^d$  [cf. Eq.(2.13)]. Fortunately, a straightforward calculation using the definition of the covariant derivative  $D$  in terms of  $\nabla$ , as well as the definition of 3-vectors in terms of 4-vectors, shows that both definitions coincide. Thus, we do not need to introduce different notation for both expressions. This coincidence is due to the skew symmetry of the Faraday's tensor. An inconsistency would arise, however, if one were to define the 3-Riemann tensor as in Eq. (2.13). We know that the projection of the 4-Riemann tensor onto  $\Sigma_t$  as in Eq. (2.13) is in fact related to the 3-Riemann tensor through one of the Gauss-Codazzi equations. Had one used the same notation for both 3-tensors, or identified one with the other, a serious inconsistency would arise. Therefore, special care has to be taken when using the notation with  ${}^{(3)}$  within a projected tensor which arises originally from covariant derivatives of 4-tensor fields. The point is that the spatial components of 4-tensors do not necessarily coincide with the spatial components of the corresponding 3-tensors. In the case of the 4-Riemann tensor it is obvious that its spatial components involve time components of Christoffel symbols and therefore, time components of the metric. Whereas the 3-Riemann tensor involves the 3-metric solely. In the case of the Faraday's tensor the spatial covariant components coincide in both cases.
- [52] The Eulerian observers are called also *fiducial observers* [28], or even ZAMO observers [45], in the case of stationary and axisymmetric spacetimes. ZAMO stands for *zero angular momentum observers* because their angular momentum  $L := n^a \psi_a$  turns out to be identically zero. Here  $\psi^a = (\partial/\partial\phi)^a$  stands for the rotational Killing vector field which generates the isometries around the axis of symmetry.
- [53] It is easy to see that any tensor  $T_{a_1\dots a_{q-1}}$  of type  $(0, q-1)$  defined as the contraction of  $n_a$  with a totally antisymmetric tensor  $A_{a_1\dots a_q}$  of type  $(0, q)$  will in turn be a 3-tensor by the same argument. This is exactly what happens in Eqs. (2.18) and (2.19).
- [54] In a similar fashion we can define  ${}^{(3)}\epsilon_{\perp efg} = {}^{(3)}\epsilon_{efg}$  such that  ${}^{(3)}\epsilon_{123} = +\sqrt{h}$ . Indeed  $\epsilon_{\perp acd} := n^b \epsilon_{bacd}$ , and therefore  $\epsilon_{\perp 123} = (1/N) \epsilon_{0123} = \sqrt{h}$  (where  $\epsilon_{0123} = +\sqrt{-g} = N\sqrt{h}$ ).
- [55] Substituting Eqs. (2.23) and (2.24) in Eq. (2.28), one obtains  $F^{ab} = n_c \epsilon^{abcd} B_d + n^a E^b - E^a n^b$ , which is in fact the second of Eqs. (3.2) of Thorne & Macdonald [28].
- [56] In the left-handed convention one has  $\epsilon^{0123} = +1/\sqrt{-g}$  and  $\epsilon_{0123} = -1\sqrt{-g}$ . One should then take the definition  ${}^{(3)}\epsilon^{\perp afg} := -n_b h^a_e h^f_c h^g_d \epsilon^{abcd}$ , so that  ${}^{(3)}\epsilon^{\perp efg}$  is always positive and therefore independent of the conventions. Namely,  ${}^{(3)}\epsilon^{\perp 123} = N\epsilon^{0123} = +1/\sqrt{h}$ . In this way the signs of Eqs. (2.22) and (2.27)–(2.29) remain invariant, as well as the subsequent derivations which use them, like Maxwell's equations.
- [57] This equation can also be written in the following way  $\partial_t \vec{E} + \mathcal{L}_N E^i = D_{\text{flat}} \times (N \vec{B}) + NK \vec{E} - 4\pi N {}^{(3)}\vec{j}$ , with  $N := N/\sqrt{h}$  the densitized lapse, and where the rotational operator is that of flat space (even if one is using curvilinear coordinates). The curvature and geometric factors have been absorbed in the densitized lapse.
- [58] In order to compare equations (3.4a)–(3.4d) of Thorne & Macdonald [28] with ours we must translate their notation to ours as follows:  $U_\alpha \rightarrow n_a$ ,  $\theta \rightarrow -K$ ,  $\sigma_{\alpha\beta} \rightarrow -(K_{ab} - \frac{1}{3}Kh_{ab})$  which corresponds to minus the traceless part of the extrinsic curvature;  $\tilde{\nabla} \rightarrow D$ ,  $\alpha \rightarrow N$ ,  $D_\tau M^\beta \rightarrow n^a \nabla_a M^b - M_a a^a n^b$  [cf. their Eq. (2.12)] where in the present case  $M^a$  stands for  $E^a$  or  $B^a$ . When multiplied by  $N$  the terms  $n^a \nabla_a M^b - M_a a^a n^b$  can be easily arranged to give the first term on the l.h.s of Eq. (2.33) or the first two terms on the l.h.s of Eqs. (2.37) and (2.38). In general a tilde used by those authors under several quantities or symbols stands for quantities defined on  $\Sigma_t$ , whether they are 3-vectors or derivatives compatible with the 3-metric.
- [59] In Fourier space the system reads  $\omega \hat{u} - M^i k_i \hat{u} = \hat{\mathcal{S}}$ .
- [60] Modulo notation, Eqs. (2.75)–(2.77) coincide exactly with Eqs (3.10) of Thorne & Macdonald [28].
- [61] See Refs. [34, 46, 47], for a review and discussion on the initial value problem of the Einstein-Maxwell system.
- [62] In Schwarzschild (area) coordinates the Reissner-Nordström solution is given by  $ds^2 =$

$$-\left(1 - \frac{2M}{\bar{r}} + \frac{Q}{\bar{r}^2}\right) dt^2 + \left(1 - \frac{2M}{\bar{r}} + \frac{Q}{\bar{r}^2}\right)^{-1} d\bar{r}^2 + \bar{r}^2 d\Omega^2.$$

[63] In order to recover the physical electric field for this static solution, one has to remember the definition (2.18), so that  $E_a = -n^b F_{ba}$ . Since in this case the spacetime is static we have  $n^a = (1/N)(\partial/\partial t)^a$ , where  $(\partial/\partial t)^a$  is the timelike Killing vector field which is hypersurface orthogonal. Then  $E_a = -(1/N)F_{ta} = (1/N)\partial_a A_t$ . Using Eq. (3.27) one has  $E_a = \psi^2 \partial_a A_t$ . From Eqs. (3.8)

and (3.13) one obtains  $\partial_a A_t = -\psi^{-4} \partial_a \varphi$ . Finally using  $\psi^2 = 1 + \varphi$  [cf. Eqs. (3.22) and (3.26)] one concludes  $A_t = \text{const.} + (1 + \varphi)^{-1} = \text{const.} + \psi^{-2}$ , where the integration constant can be fixed in several ways. In the standard form of Papapetrou and Majumdar the constant is usually fixed to be zero. However one can choose it equal to -1 if one demands that  $A_t$  vanish asymptotically.